General view on the progress in nuclear fission : a review

Karl-Heinz Schmidt, Beatriz Jurado

General view on the progress in nuclear fission: a review

Karl-Heinz Schmidt, Beatriz Jurado

CENBG, CNRS/IN2 P3, Chemin du Solarium B.P. 120,
F-33175 Gradignan, France

May 4, 2016

Abstract: An overview is given on some of the main advances in experimental methods, experimental results and theoretical models and ideas of the last years in the field of nuclear fission.

New approaches extended the availability of fissioning systems for experimental studies of nuclear fission considerably and provided a full identification of all fission products in A and Z for the first time. In particular, the transition from symmetric to asymmetric fission around ^{226}Th and some unexpected structure in the mass distributions in the fission of systems around $Z = 80$ to 84 as well as an extended systematics of the odd-even effect in fission fragment Z distributions have been measured.

Three classes of model descriptions of fission presently appear to be the most promising or the most successful ones: self-consistent fully quantum-mechanical models, stochastic models, and a new semi-empirical model description.

The first ones are the only ones that fully consider the quantum-mechanical features of the fission process. Unfortunately, the most advanced models in nuclear physics that have been developed for stationary states are not readily applicable to the decay of a meta-stable state. Intense efforts are presently made to develop suitable theoretical tools. Moreover, the technical application of the most advanced models is heavily restricted by their high demand on computer resources.

Stochastic models provide a fully developed technical framework. The

main features of the fission-fragment mass distribution were well reproduced from mercury to fermium and beyond. However, the limited computer resources still impose severe restrictions, for example on the number of collective coordinates.

In an alternative approach, considerable progress in describing the observables of low-energy fission has been achieved by exploiting powerful theoretical ideas based on fundamental laws of mathematics and physics. This approach exploits (i) the topological properties of a continuous function in multidimensional space, (ii) the separability of the influences of fragment shells and macroscopic properties of the compound nucleus, (iii) the properties of a quantum oscillator coupled to the heat bath of the other nuclear degrees of freedom for describing the fluctuations of normal collective modes, and (iiii) an early freeze-out of collective motion to consider dynamical effects.

This new approach reveals a high degree of regularity and allows calculating high-quality data that are relevant for nuclear technology without specific adjustment to experimental data of individual systems.

1 Introduction

The discovery of fission revealed that the heaviest nuclei are barely bound in their ground state. An excitation energy in the order of a few percent of their total binding energy is sufficient to induce the disintegration into two pieces in a collective shape evolution that resembles the division of living cells, releasing a huge amount of energy of about 200 MeV. Thus, the specific energy content of nuclear fuel is about 10^8 times larger compared to fossil fuels like coal, mineral oil or natural gas. This explains the importance of fission in nuclear technology.

The energy stored in heavy nuclei, and even the synthesis of an appreciable portion of matter in the Universe has its origin in the astrophysical r-process, a process of consecutive neutron capture and beta decay in an environment with a very high neutron flux in some astrophysical site, which is not yet fully identified [1]. Fission is believed to play an important role in the r-process itself by fission cycling that limits the mass range of the r-process path and has an influence on the associated nuclide abundances [2]. Therefore, additional interest for a better understanding of the fission properties of nuclei far from stability comes from astrophysics.

In a general sense, nuclear fission offers a rich laboratory for a broad variety of scientific research on nuclear properties, astrophysics and general

physics. The r-process nucleosynthesis cannot be fully understood without a precise knowledge of the fission properties of very neutron-rich isotopes of the heaviest elements, which are presently not accessible to direct measurements [3]. The relatively flat potential energy reaching to very large deformations allows studying nuclear properties like shell effects in super- and hyper-deformed shapes [4]. Phenomena connected with the decay of the quasi-bound nuclear system beyond the fission barrier yield information on nuclear transport properties like nuclear viscosity [5, 6] and heat transfer between the nascent fragments [7]. They even offer a valuable test ground of general importance for non-equilibrium processes in isolated mesoscopic systems, where quantum mechanics and statistical mechanics play an important role [8].

During the last years there has been a considerable activity in the field of nuclear fission, both experimental and theoretical. Several detailed and some comprehensive papers have been written on the development of theoretical approaches and formalisms. From the experimental side there have been publications on refinements of existing or the development of novel techniques as well as on new experimental findings. Usually, the technical development of the specific theoretical or experimental approach, its challenges and achievements, are in the focus of these papers. Theoretical papers often intend to demonstrate the quality of a specific approach by showing its ability for reproducing some distinct data and to present computational algorithms that provide suitable approximate descriptions when exact solutions are out of reach, which is often the case. Experimental work is often driven by the interest for reliable nuclear data that are required for some technical applications.

The present review article has a different goal. It aims at promoting an improved understanding of the nuclear-fission process by establishing a synopsis of different theoretical approaches and of empirical knowledge on a general level. Its impetus lies in tracing back experimental findings to the underlying physics on different levels, reaching from microscopic descriptions to fundamental laws of statistical mechanics while covering essentially all fission quantities.

We will concentrate on low- and medium-energy fission, where binary fission is the dominant decay channel with two heavy fragments. Ternary fission with its very specific features is not included. A compact but rather exhaustive record on the most relevant experimental and theoretical work in this field is given in the introduction of ref. [9]. The decay of highly excited nuclei, where the phase space favors multifragmentation [10, 11], the simultaneous decay into more than two fragments, and quasi-fission [12]

after heavy-ion reactions that preserve a memory on the entrance channel are not covered neither. Also for the description of fission cross sections and fission probabilities in induced fission that involves the entrance channel, the transmission through the fission barrier and the competition with other exit channels, we refer to dedicated papers [13, 14, 15, 16].

The present article is structured as follows. After a short reminder on the former status of knowledge in section 2, we will give a review on the recent innovations in experimental and theoretical work in sections 3 and 4, respectively. Major steps in experimental fission research were made during the last years by the application of inverse kinematics and the observation of beta-delayed fission. On the theoretical side, fully dynamical descriptions of the fission process in quantum-mechanical and classical models are being developed. Moreover, the application of a number of general laws and ideas delivered very interesting explanations or opened well targeted questions for some prominent and some very peculiar observations that stayed unexplained for long time or that emerged from the results of recent experiments. A general discussion of current problems that covers experimental results and different theoretical models and ideas is provided in section 5, followed by an outlook on further progress in experimental and theoretical research.

In the interest of the comprehensive and consistent discussion in section 5, section 2 does not include former experimental results that were interpreted only recently in the framework of new theoretical ideas. In a similar way, section 4 presents predominantly the basic and the technical aspects of the different models.

2 Former status of knowledge

Since the discovery of nuclear fission, the bulk of the experimental results has been obtained in neutron-induced fission of available and manageable target nuclei. Limitations arise from the small number of primordial or long-lived heavy target nuclides and from the technical difficulties of experiments with monoenergetic neutrons of arbitrary energy. Therefore, for example the majority of the experiments on fission yields has been made with thermalized reactor neutrons and, to a lesser extent, with fast neutrons and neutrons of 14 MeV. Moreover, in all experiments performed in direct kinematics, the kinetic-energies of the fission products are hardly sufficient for obtaining an unambiguous identification of the fission products in A *and* Z in kinematical measurements, which implies that complete fission-product distributions

cannot be provided.

An exhaustive overview of the experimental results on neutron-induced fission is given in a recent review by Gönnenwein [17]. It essentially covers fission cross sections, the fission-product mass distributions, kinetic and excitation energies, nuclear-charge distributions of the lighter fission products and in particular the odd-even staggering, and the emission of prompt neutrons and gammas.

Also many experiments on charged-particle-induced fission [18] and photon-induced fission (bremsstrahlung or monoenergetic photons), e.g. ref. [19] and references therein, have been and are still being performed. The use of charged-particle or heavy-ion projectiles made a number of additional nuclei available for fission experiments by transfer reactions [20] or fusion (e.g. refs. [21, 22]). The easy accessibility of higher excitation energies and the inevitable population of larger angular momenta allow to study other aspects of the fission process. They are described in the recent review by Kailas and Mahata [18] and not covered in this work.

The prominent theories developed in parallel with these observations provided potential-energy surfaces of the fissioning systems in macroscopic-microscopic or self-consistent fully microscopic approaches. Structures in fission-fragment mass and nuclear-charge distributions were analyzed with the multi-modal fission model of Brosa et al. [23] and the combinatorial model of Nifenecker et al. [24], respectively, but they rather remained on a level of empirical parametrization.

While only qualitative considerations on the dynamical evolution of the fissioning system at low excitation energies could be made, see e. g. the S-matrix formulation of Nörenberg [25], Wilkins et al. [26] performed already quantitative calculations of fission quantities with a static statistical scission-point model, including the influence of shell effects and pairing correlations. Although this model disregards any influence of the dynamics, which prevents for example obtaining any information on dissipation, successors of this model are still being developed [27, 28, 29], often achieving a good reproduction of measured mass distributions and other quantities, for example for thermal-neutron-induced fission of ^{232}Th, ^{235}U, ^{239}Pu, and ^{245}Cm [27], and for spontaneous fission of nuclei around ^{258}Fm and above [29].

3 Experimental innovations

There has been a continuous progress in the quality of experimental equipment by the development in technology on many fields. This allowed to improve the quality and to extend the quantity of experimental results in many aspects. As a direct consequence, the data basis for applications in nuclear technology has considerably improved. In the present section, we give a concise overview on only a few major developments that gave a considerably improved insight into the physics of the fission process. A comprehensive and detailed overview on technological developments and new experimental results is presented in a dedicated review that appears in parallel [30].

3.1 Accessible fissionable nuclei

The progress in the understanding of fission heavily relied and still relies on the development of advanced experimental methods. A severe restriction is still the availability of fissionable nuclei as target material. Therefore, the traditional use of neutrons for inducing fission offers only a rather limited choice of fissioning systems. These limitations were more and more overcome by alternative methods: For instance, spontaneously fissioning heavy nuclei are being produced by fusion reactions since many years, as already mentioned.

Recently, very neutron-deficient nuclei, e.g. in the $Z = 80$ region, were produced in spallation reactions at ISOLDE, which undergo beta-delayed fission [31]. This experiment profited from an unambiguous identification of the fissioning nuclei, mass selection by ISOLDE and Z selection by the resonance ionization laser ion source RILIS. A pronounced double-humped mass distribution was found for the fission fragments of the compound nucleus ^{180}Hg, which has similarities with the double-humped mass distribution observed previously by Itkis et al. [32] for the fission of excited ^{201}Tl that is situated close to beta stability in an alpha-induced reaction. Some structure in the mass distribution was also observed for the fission of ^{194,196}Po and ^{202}Rn. In addition to the papers cited in ref. [31], these unexpected observations in beta-delayed fission triggered several experiments with different techniques [33, 34, 35, 36] and a number of theoretical works [37, 38, 33, 39, 40], which could reproduce the observed features to a great extent.

Advanced experimental studies on light-charged-particle-induced fission probabilities of systems that are not accessible by neutron-induced fission are being performed systematically. These surrogate-reaction studies focus on the ability of these alternative reactions to simulate neutron-induced re-

actions [41]. Also recently, the use of heavier ions, for example ^{16}O, in transfer reactions allowed to appreciably extend the range of fissionable nuclei available for fission studies [42]. Moreover, comprehensive studies on fission of transfer products of ^{238}U projectiles, impinging on a ^{12}C target, have been performed in inverse kinematics, covering fission probabilities [43] and fission-fragment properties [44].

Fragmentation of relativistic ^{238}U projectiles made a large number of mostly neutron-deficient projectile fragments with $A \leq 238$ available for low-energy fission experiments in inverse kinematics by electromagnetic excitations [45, 46, 47]. When fission events after nuclear interaction are suppressed, the excitation-energy distribution centers at about 14 MeV above the ground state with a FWHM of about 5 MeV.

3.2 Boosting the fission-fragment kinetic energies

The identification of fission products poses a severe problem. First experiments were based on radiochemical methods [48, 49]. This approach is not fast enough for determining the yields of short-lived fragments, and it suffers from normalization problems. Identification with kinematical methods by double time-of-flight [50, 51] and double-energy measurements [52] provide complete mass distributions, however with limited resolution. At the expense of a very small detection efficiency, the COSI-FAN-TUTTE set-up [53, 54] had some success in measuring mass and nuclear charge of fission fragments at high total kinetic energies in the light group by combining double time-of-flight, double-energy and energy-loss measurements. The LOHENGRIN spectrograph brought big progress in identifying the fission products in mass and nuclear charge [55], although the Z identification was also limited to the light fission-product group. This technique was applied to thermal-neutron-induced fission of a number of suitable targets that were mounted at the ILL high-flux reactor. Recent attempts for developing COSI-FAN-TUTTE - like detector assemblies with higher detection efficiency and better resolution are presently being made, but showed only limited success up to now [56, 57, 58, 59, 60]. In particular, the Z resolution is severely impeded by straggling phenomena.

Full nuclide identification (in Z and A) of *all* fission products has only been achieved by boosting the energies of the products in inverse-kinematics experiments and by using powerful magnetic spectrometers [45, 46, 47, 61, 62].

3.3 Results

Some of the most prominent new results have been obtained in fission experiments performed in inverse kinematics on electromagnetic-induced fission at relativistic energies [45, 47] and on transfer-induced fission at energies slightly above the Coulomb barrier [44].

In ref. [45], the fission-fragment Z distributions of 70 fissionable nuclides from ^{205}At to ^{234}U were measured, using beams of projectile fragments produced from a 1 A GeV ^{238}U primary beam and identified by the fragment separator of GSI, Darmstadt. The measured Z distributions show a gradual transition from single-humped to double-humped distributions with increasing mass, with triple-humped distributions for fissioning nuclei in the intermediate region around $A = 226$. The position of the heavy component of asymmetric fission could be followed over long isotopic chains and turned out to be very close to $Z = 54$ for all systems investigated. In a refined analysis, it was shown that the mean Z values of the contributions to the heavy component from the two most prominent asymmetric fission channels are nearly the same for all actinides [63]. Moreover, the odd-even structure in the Z yields was found to systematically increase with asymmetry and to have similar magnitudes for even-Z and for odd-Z fissioning nuclei at large asymmetry [64, 65]. The importance of these findings for the theoretical understanding of the fission process is further discussed in sections 4.3.2 and 4.3.3.

The SOFIA experiment [46, 47] that used a refined and extended set-up compared to the one used in ref. [45] allowed to fully identify unambiguously event by event all fission products in Z *and* A from electromagnetic-induced fission of relativistic ^{238}U projectiles. The experiment profited also from the higher available beam intensity.

As one of the most prominent results, this experiment showed for the first time that the fine structure in the fission-product N distribution depends only weakly on the excitation energy of the fissioning system, in contrast to the odd-even staggering in the Z distribution. This can be seen in figure 1, where the logarithmic four-point differences[1], $\delta_n(N + 3/2) = 1/8(-1)^{N+1}(\ln Y(N + 3) - \ln Y(N) - 3[\ln Y(N + 2) - \ln Y(N + 1)])$, of the fission-fragment N distribution from the SOFIA results for electromagnetic-induced fission of ^{238}U are compared with those obtained for thermal-neutron-

[1]The logarithmic four-point difference [66] quantifies the deviations of a distribution from a Gaussian function, see section 4.3.3. It is used to determine the local odd-even staggering [69], but it contains also other contributions, for example from fine structures due to shell effects and from a kerf between different fission channels.

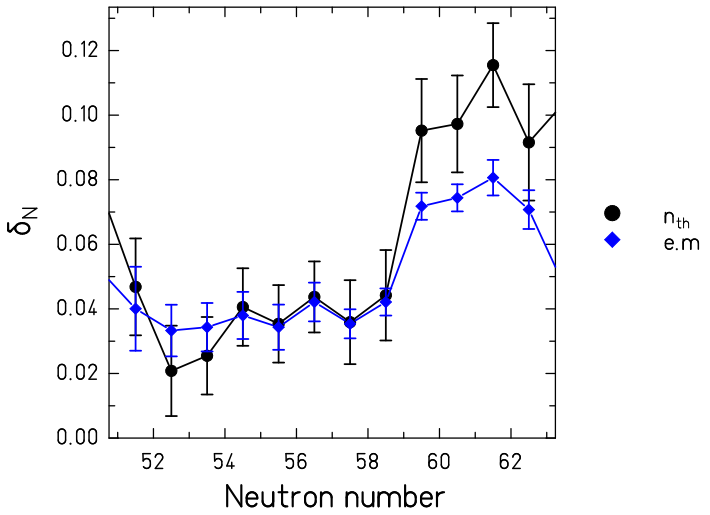

Figure 1: (Color online) Logarithmic four-point differences δ_n [66] in the fission-fragment neutron-number distribution for electromagnetic-induced fission of ^{238}U measured in the SOFIA experiment [67] and in thermal-neutron-induced fission of ^{235}U [68]. The figure shows the most relevant data in the range that contains about 90% of the N distribution of the system ^{235}U(n$_{th}$,f).

induced fission of ^{235}U.[2] Around the maximum of the N distribution at $N \approx 56$, the δ_N values are almost identical, and they are fairly close below and above $N = 56$. In contrast, the odd-even staggering in the Z distribution decreases by about 50% [65] when comparing electromagnetic-induced with thermal-neutron-induced fission. See section 4.3.3 for further discussion of the fine structure in the fission-fragment yields.

Also in the VAMOS experiment on transfer-induced fission around the Coulomb barrier in inverse kinematics, a separation in Z and A of all fission products was obtained [70], although the peaks showed some overlap,

[2]Unfortunately, there are no data available yet that allow comparing the N distributions for the same fissioning nucleus. However, the neutron separation energies, which are believed to be at the origin of the odd-even staggering in neutron number, see ref. [185] and section 4.3.3, vary only little along the slight displacement in the fission-fragment Z distributions for a fixed N. Moreover, a direct comparison is anyhow not possible due to the presence of multi-chance fission in the SOFIA experiment.

preventing an unambiguous event-by-event identification. This experiment also provided for the first time complete fission-product nuclide distributions after the formation of a ^{250}Cf compound nucleus at an excitation energy as high as 45 MeV, produced in the fusion of ^{238}U projectiles with ^{12}C [70] and a number of transfer products [71]. This allowed, for the first time, to systematically study the dependence of the N/Z degree of freedom (charge polarization and fluctuations), on excitation energy [70, 72, 71], regarding that the full nuclide identification had previously been obtained for the light fission products from thermal-neutron-induced fission of a small number of fissioning systems, only.

The observation of a double-humped mass distribution in the fission of the very neutron-deficient ^{180}Hg nucleus in beta-delayed fission and different kind of structure in the mass distributions from fission of other nuclei in this region in different experiments demonstrated that complex structural effects are a rather general phenomenon in low-energy fission, not restricted to asymmetric fission in the actinides and multi-modal fission around ^{258}Fm. This result demonstrates that, contrary to the symmetric fission in neutron-rich Fm isotopes, which is explained by the simultaneous formation of two fragments close to the doubly-magic ^{132}Sn, the production of two semi-magic ^{90}Zr fragments is not favored in this case. A large variety of neutron-deficient nuclei reaching down even below mercury is also accessible to fission studies at energies close to the fission barrier with the SOFIA experiment. A few exploratory measurements have already been made [73].

4 Theoretical innovations

In the following, we will give a survey on the ability of different newly developed theoretical approaches and ideas to closely reproduce experimental observables and to reveal the physics behind. Because the dynamics of the fission process and the influence of shell effects and pairing is considered to be essential assets for the understanding of low-energy fission, static and purely macroscopic approaches are not included. The survey comprises microscopic self-consistent approaches, stochastic models and ideas based on general laws of mathematics and physics.

The reader who is interested in an exhaustive overview on the current status of microscopic fission theory that is covered in the sections 4.1 and 4.2 can find it, among other topics, in the recently published textbook of Krappe and Pomorski [74].

4.1 Microscopic self-consistent approaches

The most ambitious theoretical approaches to nuclear fission aim at describing the fission process on the basis of the nuclear force, may be even derived from QCD [75]. Due to the tremendous number of possible final configurations, the fissioning system must be treated as an open system, where only a sub-class of the degrees of freedom associated to the system that are considered to be relevant are of direct interest. Usually, these are some of the collective degrees of freedom. The other degrees of freedom are attributed to an environment and not explicitly followed. One of the major difficulties is the necessity to treat collective and single-particle degrees of freedom simultaneously as quantum objects [76]. Moreover, fission is a dynamical process and it should be treated as such.

Table 1 shows a list of dynamical self-consistent quantum transport theories that have been developed for handling nuclear reactions. The application to nuclear fission poses considerable challenges on suitable algorithms and computation resources and is presently an active field of development. At present, only part of these approaches has been applied to fission. The table has been prepared on the basis of table 1 presented in the habilitation thesis of D. Lacroix [77]. We also refer to this thesis for a detailed description of the different methods and the appropriate references. Here, we only intend to give an overview on the variety of sophistication and the challenges self-consistent fission theory is facing.

Table 1: Some dynamical self-consistent microscopic approaches

Name	approximation	associated observable
TDHF	mean-field (m.-f.)	one-body
TDHF-Bogoliubov (TDHFB)	m.-f. + pairing	generalized one-body
TD generator coordinate meth. (TDGCM)	m.-f. + pairing	generalized one-body
Extended TDHF (ETDHF)	m.-f. NN collisions (dissipation)	one-body
Stochastic TDHF (STDHF)	m.-f. + NN collisions (dissipation+fluctuations)	one-body
Stochastic mean-field (SMF)	m.-f. initial fluctuation	conf. mixing
Time-dept. density matrix (TDDM)	m.-f. + two-body correlations	one- and two-body
TDGCM + SCIM Schrödinger collective intrinsic Model	m.-f. + pairing + dissipation	one- and two-body
Time-dept. energy-density functional (TD-EDF)	mean-field	one-body
Time-dept. superfluid local density approx. (TDSLDA)	m.-f. + pairing	generalized one-body
Beyond mean-field TD-EDF	m.-f. + two-body correlations	one- and many-body
Quantum Monte-Carlo (QMC)	exact (within stat. errors) quantum jump	all

Note: This table is based on table 1 in the habilitation thesis of D. Lacroix [77]. In the present table we make a distinction between TDHF and TD-EDF, but very often in literature one uses the term TDHF for calculations that are actually based on the TD-EDF technique, see ref. [78]. The last column specifies the nature of the associated degrees of freedom.

Time-dependent Hartree-Fock (TDHF) theory considers the evolution of the nucleonic wave functions in a mean field that is itself determined by the wave functions, whereby direct interactions between the nucleons are neglected. More elaborate approaches include pairing correlations (e.g. TDHF-Bogoliubov (TDHFB)), or other kind of many-body interactions in different levels of approximation. The generator coordinate method is a method that is used to determine the dynamic evolution of the wave functions along the fission path. Only few allow for dissipation, an energy exchange between the relevant degrees of freedom and the environment, on different levels of sophistication. The Schrödinger Collective Intrinsic Model is one of the most elaborate approaches of this kind that has been applied to fission. The Quantum Monte-Carlo approach provides an exact solution of the evolution of the subsystem of selected variables in an environment with fluctuations. The application is limited by numerical difficulties. The energy-density functional (EDF) theory corresponds essentially to the replacement of the initial complex many-body problem by an energy functional of the density. It simplifies the solution of the problem in many cases.

In practice, an application to fission dynamics is generally performed in two steps. In a first step, the potential energy and eventually the collective inertia in the space spanned by the degrees of freedom that are considered to be relevant is computed. For this purpose, the energy of the system is determined under the constraint of the coordinates of the relevant degrees of freedom on a grid of points. In each point, the shape of the system is optimized in a self-consistent way with respect to its energy while respecting the imposed constraints. In a second step, the time-dependent evolution of the system is determined by some of the suitable dynamical methods listed in table 1. Some drawbacks of this procedure are discussed in section 5.1.2. These are overcome in the time-dependent superfluid local density approximation (TDSLDA) [79], where, besides an elaborate treatment of pairing correlations, the evolution of the system with all ingredients as potential energy, collective excitations and kinetic energy are calculated in one passage in a self-consistent way without any constraints.

Some self-consistent dynamical calculations on spontaneous fission have been performed. For example, Staszczak et al. [80] studied the multimodal spontaneous fission of isotopes from californium to hassium with the nuclear density functional theory, considering elongation, reflection asymmetry, necking and triaxiality as the relevant shape degrees of freedom. Sadhukhan et al. [81] determined the spontaneous-fission half life of ^{264}Fm and ^{240}Pu with the nuclear density functional theory by minimizing the collective action integral for fission in a two-dimensional quadrupole collective space

representing elongation and triaxiality and demonstrated the influence of pairing correlations on the fission path.

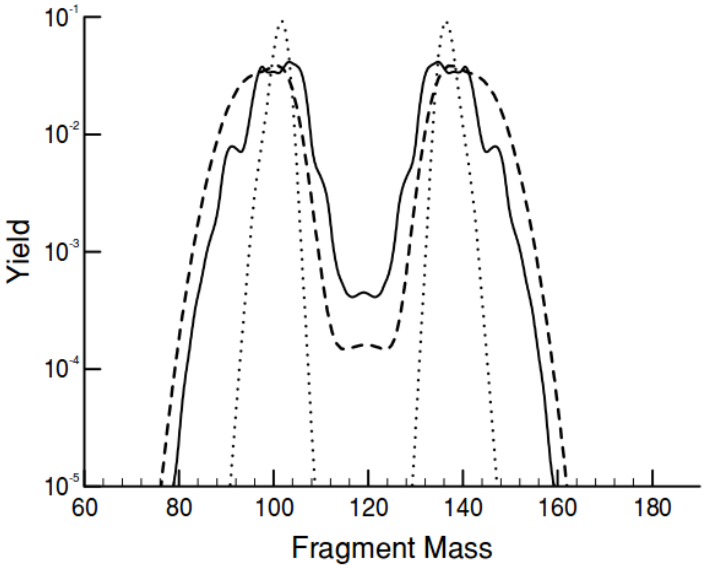

Figure 2: Comparison between the calculated one-dimensional mass distribution (dotted line), the mass distribution resulting from the dynamic calculation (solid line) with the initial state located 2.4 MeV above the barrier, and the Wahl evaluation (dashed line) [83]. The calculation has been performed with the TDGCM approach [82]. The figure is taken from ref. [82].

With a self-consistent Hartree-Fock-Bogoliubov procedure, Goutte et al. [82] calculated mass- and kinetic-energy distributions of the fragments produced in low-energy fission of ^{238}U for excitation energies slightly above the fission barrier. The Gaussian overlap approximation of the time-dependent generator coordinate method (TDGCM) was used and adiabaticity[3] was assumed. By applying constraints on the quadrupole and octupole moments, the elongation and the mass asymmetry were considered to be the two relevant parameters of the fissioning systems. As shown in figure 2, the broadening of the mass distribution by dynamical effects is demonstrated by a comparison with a one-dimensional static calculation, where collective

[3]In the present context, adiabaticity means that the quantum states remain unchanged during the course of the reaction

stationary vibrations are studied along the sole mass-asymmetry degree of freedom for nuclear configurations just before scission. Simenel and Umar [84] studied dynamical effects on the kinetic and excitation energies of the fragments in symmetric fission of ^{258}Fm and ^{264}Fm with time-dependent-Hartree-Fock calculations, including non-adiabatic processes in the vicinity of scission. This approach has been extended by including pairing correlations by Scamps et al. [85] and applied to multi-modal fission of ^{258}Fm. The importance of dissipation in the early stage of the evolution close to the fission barrier is exemplified for symmetric fission of ^{258}Fm by Tanimura et al. [86] by time-dependent energy density functional (TD-EDF) theory, although this approach suffers from an approximate treatment of pairing correlations that hinders the adjustment of occupation probabilities of magnetic sub-states.

Another essential step towards a full dynamical microscopic description of the fission process is the generalization of the TDGCM approach by including two-quasiparticle excitations on the whole fission path in the Schrödinger Collective Intrinsic Model (TDGCM + SCIM) by Bernard et al. [87].

A further very interesting aspect is the quantum localization of the nucleonic wave functions inside the nascent fragments around scission. Quantum localization in fission has first been studied by Younes et al. [88] with the HFB method with one constraint on the quadrupole moment as a function of a constraint on the neck size that represents the scission process. An extended investigation of quantum localization in the scission configuration at zero temperature has been performed by Schunk et al. [89] based on the EDF approach with Skyrme energy densities. This last study has been extended to finite temperature in ref. [90]. These studies, wich are presently still static in nature, are a pre-requisit for describing the dynamical evolution of the fissioning system around scission on a quantum-mechanical basis regarding the non-locality of the many-body wave function of the nucleus and without assuming an arbitrarily defined scission point. Incorporated in a full-scale dynamical approach of the fission process, they will allow to model the process in which the fragments acquire their individual characteristics and the fast evolution of the intrinsic structure of the fissioning system during the violent shape change at scission.

Very recently, Bulgac et al. solved a common problem of many dynamical self-consistent approaches that do not allow the system to evolve to fission, unless the calculation started far beyond the outer saddle (e.g. [78, 85, 86]) or with an initial boost (e.g. [86, 91]). This was achieved in their TDSLDA model [79] by allowing transitions between magnetic sub-states during the

dynamic evolution of the system by means of a complex pairing field that varies in time and in space. They presented rather precise calculations of some specific average fission quantities (fragment excitation energies, kinetic energies, saddle-to-scission time) in thermal-neutron-induced fission of ^{239}Pu. Long fission times are obtained due to the excitation of a large number of collective degrees of freedom, confirming early qualitative results of Nörenberg [25].

At present, the importance of microscopic self-consistent models for the description of nuclear fission lies in the qualitative understanding of several fundamental aspects, while the achievements in completeness and precision are in a vivid process of development. The precision of microscopic self-consistent calculations depends essentially on the nuclear force. For example, a good reproduction of the empirical fission barriers is still a challenge, see ref. [92]. Presently, the predicted fission-barrier heights of very neutron-rich nuclei are still rather sensible to the nuclear force [93]. Only a limited variety of fission observables, mostly spontaneous-fission half lives, fission-fragment mass distributions and kinetic energies, are treated up to now. The practical restrictions due to the very high demand on computing power are still severe. In the long term, microscopic self-consistent models are expected to be particularly strong in reliable predictions for exotic systems that are not accessible to experimental studies.

4.2 Stochastic approaches

Early dynamical studies of the nuclear fission process have been performed by Nix [94] with a non-viscous irrotational liquid-drop model and by Davies et al. [95] with the inclusion of two-body dissipation. Later Adeev et al. [96] studied the influence of one-body and two-body dissipation on the fission dynamics with a transport equation of the Fokker-Planck type. Also in this case, like in the microscopic self-consistent approaches, only a limited part of the large number of degrees of freedom is explicitly treated. In ref. [96], the evolution of the probability-density distribution in a space defined by the restricted number of degrees of freedom that are considered to be relevant is described under the influence of a driving force and friction, including the associated statistical fluctuations. Driving force and friction represent the interactions with the other degrees of freedom that are not explicitly considered. However, the solution of the Fokker-Planck equation was limited to simple cases or subject to strong approximations. Abe et al. [97] replaced the Fokker-Planck equation by the equivalent Langevin equations that can be solved numerically. Monte-Carlo sampling of individual trajectories in

the space of the relevant degrees of freedom proved to be a more practicable way for obtaining more accurate solutions in complex cases. However, this method requires considerable computing resources.

The Langevin equations in their discretized form for the evolution of the system in the time interval Δt between the time step i and $i+1$, reads

$$q_{i+1} = q_i + \frac{p_i}{m}\Delta t \tag{1}$$

and

$$p_{i+1} = p_i - T\frac{dS}{dq}\Delta t - \beta p_i \Delta t + \sqrt{\beta m T \Delta t}\cdot\Gamma. \tag{2}$$

q is the coordinate in the space of the relevant degrees of freedom, p the corresponding momentum. m and β are the mass parameter and the dissipation coefficient, respectively. T is the temperature and S is the entropy. Both are related to the level density[4] ρ above the potential-energy surface of the system:

$$T = (\frac{d\ln(\rho)}{dE})^{-1} \tag{3}$$

and

$$S = \ln(\rho). \tag{4}$$

In most practical cases, the stochastic variable Γ that defines the fluctuating force is linked to the dissipation strength by the fluctuation-dissipation theorem [98].

Equations (1) and (2) are valid, if m and β do not depend on the coordinate q and the direction of motion. In the general case, m and β are tensors, and the Langevin equations must be adapted. For more detailed information on the application of the Langevin equations to fission and to other nuclear reactions we refer to the review article of Fröbrich and Gontchar in ref. [99].

Since a nucleus is an isolated system with fixed total energy and fixed particle number, equations (1) and (2) must be formulated in the fully microcanonical version (specified as option 1 in table 2). This entails that temperature and entropy are associated to the total energy of the system minus the local potential and the actual collective energy. This is important in applications to low-energy fission, where approximations that are often applied (specified as options 2, 3 and 4 of table 2) only badly represent the statistical properties of the nucleus. Also the influence of pairing correlations and shell effects on the binding energy *and* the level density

[4]Strictly speaking, the degeneracy of the magnetic sub-states should be considered.

Table 2: Stochastic approaches to nuclear fission

Name	approximations
Langevin equations, microcanonical	classical dynamics *
Langevin equations, not fully microcanonical **	classical dynamics * + simplified driving force or state density
Smoluchowski equation	classical dynamics * + overdamped motion
Random walk	classical dynamics * + overdamped motion + Metropolis sampling

*) Certain quantum-mechanical features can effectively be considered in the classical Langevin equations, for example shell effects in the potential energy, contribution of the zero-point motion to fluctuation phenomena, etc.
**) Different kind of approximations, for example coupling to a heat bath of constant temperature, Boltzmann statistics etc.

should be properly considered, in particular at low excitation energies. This is not so critical at higher excitation energies, where for example the use of Boltzmann statistics may be a suitable approximation. These aspects have been stressed in several places, for example by Fröbrich in ref. [100]. He also stresses that the driving force is not given by the derivative of the potential, but by the derivative of the entropy times the temperature that expresses the influence of the environment on the selected degrees of freedom according to the laws of statistical mechanics, see equation (2). Due to the complexity of the nuclear level density, this can lead to very different results.

If very strong friction is assumed, the motion becomes over-damped, and the influence of the mass tends to vanish. This case is represented by the Smoluchowski equation [99] that requires less computational expense. Even less demanding in computing resources is the replacement of the kinematic equations (1) and (2) by a random-walk approach using Metropolis sampling [101]. All these different approaches are presently in use.

In practice, the application of stochastic classical approaches is performed in two steps, like in the case of self-consistent microscopic approaches. In a first step, the potential energy is determined on a grid in the space determined by the relevant degrees of freedom, usually by the macroscopic-

microscopic model. In most cases, the relevant degrees of freedom are the coordinates of a suitable shape parametrization. Eventually, the potential energy is minimized individually on each grid point with respect to additional shape parameters. Also the dissipation tensor and the mass tensor must be defined. With these ingredients, Monte-Carlo sampling of the fission trajectories with one of the stochastic approaches listed in table 2 is performed.

To our knowledge, stochastic approaches are being applied to low-energy fission with the inclusion of structural effects since 2002. Ichikawa et al. [102] studied the fission of ^{270}Sg with three-dimensional Langevin calculations at an excitation energy of 10 MeV. The shell effects were obtained with the two-center shell model [103]. The mass tensor was calculated using the hydrodynamical model with the Werner-Wheeler approximation [104] for the velocity field, and the wall-and-window one-body dissipation [105] was adopted for the dissipation tensor. The distance of the fragment centers, the quadrupole deformation, assumed to be common to both fragments, and the mass asymmetry were chosen as shape parameters. The measured mass distribution was well reproduced, while the total kinetic energy (TKE) was overestimated. The authors stressed the strong influence of the dynamics on the mass distribution. This model has been applied in ref. [106] to study the multi-modal fission of ^{256,258,264}Fm. In ref. [107], the influence of the dissipation tensor on the fission trajectory was demonstrated.

Aritomo et al. [108] succeeded to reproduce the measured fission-fragment mass distributions and the TKE distributions of ^{234}U, ^{236}U, and ^{240}Pu before prompt-neutron emission at an excitation energy of 20 MeV fairly well with their microcanonical stochastic approach, similar to the one applied before in refs. [102, 106, 107] and using the same shape parametrization. Figure 3 shows the comparison of the calculated and evaluated mass distributions for ^{234}U. However, they failed to reproduce the transition to single-humped mass distribution towards ^{226}Th and ^{222}Th and attributed this to an insufficiently detailed shape parametrization. In particular, they concluded that the deformation parameters of the two nascent fragments should be chosen independently. In ref. [110], Aritomo et al. introduced a new shape parametrization, but sticked to 3 dimensions. They tested the model against the mass-TKE distribution for the fission of ^{236}U at an excitation energy of 20 MeV. The influence of pairing correlations that may be assumed to be weak at this energy is neglected.

The comprehensive data base of 5-dimensional potential-energy landscapes, calculated by Möller et al. [111] with the macroscopic-microscopic approach, was used by Randrup et al. as a basis for wide-spread stochas-

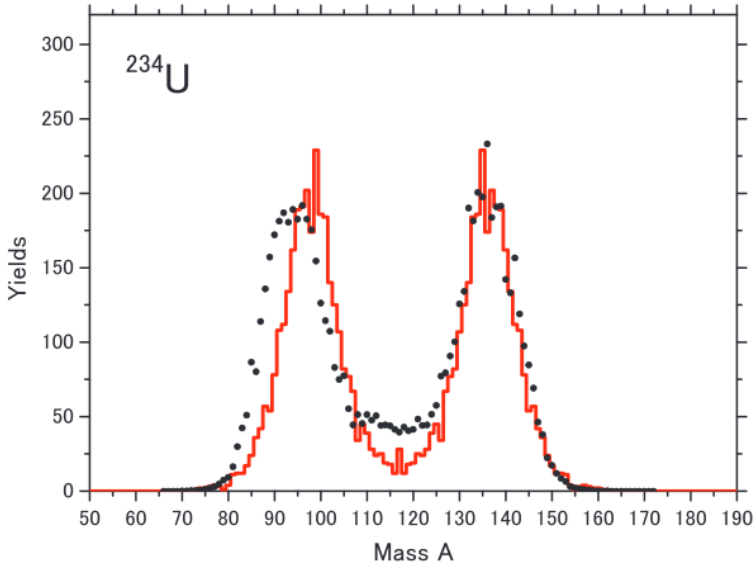

Figure 3: (Color online) Mass distribution of fission fragments of ^{234}U at $E = 20$ MeV. Calculation [108] and evaluated data [109] are denoted by histogram and circles, respectively. In contrast to the evaluated data, the calculation does not include the influence of multi-chance fission and prompt-neutron emission from the fragments. The figure is taken from ref. [108].

tic calculations of pre-neutron fission-fragment mass distributions [112, 113, 114, 115]. Z distributions were deduced with the unchanged-charge-density assumption. Due to the relatively large number of 5 shape parameters (overall elongation, constriction, reflection asymmetry, and deformations of the two individual prefragments), some simplifications and approximations in the dynamical treatment were applied in order to keep the computational needs on an affordable level. A random-walk approach using the Metropolis sampling was applied, assuming overdamped motion, and the driving force was taken as the derivative of the potential. These approximations prevent obtaining realistic results on the energetics of the fission process (for example kinetic and excitation energies of the fragments, neutron yields etc.). The measured mass distributions of a large number of systems, reaching from ^{180}Hg to ^{240}Pu are fairly well reproduced. The importance of a sufficiently detailed shape parametrization for the calculation of fission-fragment mass distributions, in particular the freedom that the nascent fragments can take

individual deformations, is demonstrated. Recently, a method to extend this approach to 6 dimensions by including the N/Z (charge polarization) degree of freedom has been proposed [116].

At present, systematic calculations of fission-fragment mass distributions for different fissioning systems have only been performed with the simplified dynamics of the Metropolis sampling [117]. Systematic calculations of fission-fragment mass distributions and total kinetic energies for many systems as a function of initial excitation energy with a fully microcanonical approach appear to be possible, but they have not yet been reported. Such results would be very interesting, although they miss the full inclusion of quantum-mechanical features. At lower excitation energies, it is necessary to consider the pairing correlations in estimating the friction tensor [118] and the mass tensor [119].

4.3 Application of general laws of mathematics and physics

Very recently, an approach to fission that exploits some general laws of mathematics and physics, combined with empirical information, has been successfully applied to develop a model, named GEF (GEneral description of Fission observables). This model covers the majority of the fission quantities and reproduces the measured observables, especially in the range $A \geq 230$, where most of the experimental data were obtained, with a remarkable precision that makes it suitable for technical applications. Many fission quantities, calculated by GEF, still pose severe problems to microscopic models. A detailed documentation of the GEF model code that is based on this approach, its underlying ideas and a presentation of a large variety of results can be found in refs. [120, 121, 122]. This approach makes use of several long-standing qualitative ideas that were already able to explain many systematic trends and regularities in several fission observables. It owes its precision and a considerable predictive power to the development of additional powerful ideas and the consideration of important experimental findings that were not fully understood before or obtained only recently. In the following, we will describe the most important ideas and their successful application in the GEF model.

4.3.1 Topographic theorem: Precise fission barriers

The modeling of the nuclear-fission process generally starts with the calculation of the potential energy of the fissioning system in the space defined by the "relevant" collective degrees of freedom. Besides the ground state of the

nucleus, the saddle point that defines the fission threshold is a prominent point in the potential-energy landscape. However, in contrast to the nuclear binding energy in the ground state, the binding energy at the fission saddle is not directly measurable. Empirical information on the fission threshold has been derived from measured energy-dependent fission cross sections and/or fission probabilities. The resulting value depends on the details of the model analysis, for example on the level-density description and, in particular, on the properties of the first excited states above the fission barrier. Therefore, the empirical fission-barrier heights are considered to be subject to an appreciable uncertainty, usually presumed to be in the order of 1 MeV, see for example ref. [92].

In this section, we will derive a well-founded estimation of this uncertainty value and propose a procedure for predicting precise fission-barrier values. This is an important information, because it allows to better assess the quality of a theoretical model by its ability to reproduce the empirical values of the fission threshold. From this result, one may conclude on the ability of the model for realistic estimations of the full potential-energy surface of the fissioning system.

Myers and Swiatecki introduced the idea that the nuclear binding energy at the fission threshold, that is the binding energy at the highest one of the consecutive barriers between the ground-state shape and the scission configuration, is influenced only little by shell effects [123], meaning that the shell-correction energy at the barrier, δU_{sad}, is small. The basic idea is illustrated in figure 4, where pairing effects are neglected, because at this stage it is assumed that the pairing condensation energy is independent of deformation and, thus, has no impact on the binding-energy difference. The height of the fission barrier B_f is given to a good approximation by the difference of the macroscopic barrier B_f^{mac} and the shell-correction energy in the ground state δU_{gs}. In practice, the ground-state shell correction δU_{gs} is determined as the difference of the ground-state energy $E_{gs-nopair}$ that is averaged over odd-even staggering in N and Z and the macroscopic binding energy: $\delta U_{gs} = E_{gs-nopair} - E_{gs}^{mac}$. If the ground-state mass is experimentally known, the fission barrier can be estimated on the basis of a macroscopic model that provides the macroscopic ground-state mass and the fission barrier, and the averaged experimental binding energy:

$$B_f \approx B_f^{mac} - E_{gs-nopair}^{exp} + E_{gs}^{mac}. \tag{5}$$

The condition for this topological property of a surface in multi-dimensional space is that the wavelength of the fluctuations induced by the shell effects

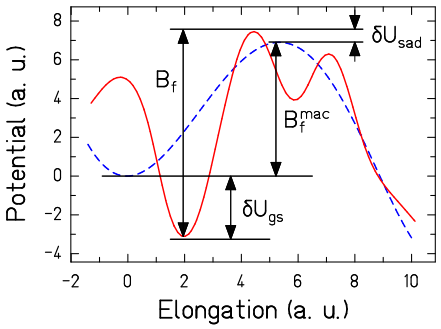

Figure 4: (Color online) Schematic drawing of the potential energy on the fission path relative to the macroscopic ground-state energy E_{gs}^{mac} for a nucleus that is deformed in its ground state. Spherical shape corresponds to zero elongation. Blue dashed line: macroscopic potential. Red full line: full potential including the shell effect. The figure is taken from ref. [124].

is smaller than the wavelength of the variations induced by the macroscopic potential. This behavior can be understood, because a local modification of the potential by a bump or a dip, for example by shell effects, does not have a big effect on the height of the saddle: The fissioning nucleus will go around the bump, and it cannot profit from the depth of the dip, because the potential at its border has changed only little. This phenomenon is related to the observation that the potential at the fission saddle in calculations with a shape parametrization tends to take lower values by allowing for more complex shapes. The inclusion of additional degrees of freedom gives access to a path that is energetically more favorable and avoids the bump mentioned above.

A detailed investigation of the applicability of the topographic theorem was performed in ref. [125]. The validity of the topographic theorem has been demonstrated before in a more qualitative way, for example in ref. [126], and possible explanations for the observed deviations in the range of a few MeV are discussed. The topographic theorem has also been used before as a test of the ability of different theoretical models to describe the long-range behavior of the fission threshold along isotopic chains [127, 128].

According to a previous analysis in [128], the average trend of the saddle mass along isotopic chains is very well reproduced by the Thomas-Fermi model of Myers and Swiatecki [123, 129]. Therefore, the comprehensive set of empirical fission thresholds, that means the maxima of the first and the

second barrier heights, from ref. [130] that are extracted from experimental fission probabilities and cross sections are compared in figure 5 with the quantity

$$B_f^{topo} = B_f^{TF} - E_{gs-nopair}^{exp} + E_{gs}^{TF} \tag{6}$$

where B_f^{TF} denotes the macroscopic fission barrier of ref. [129], represented by B_f^{mac} in figure 4, and E_{gs}^{TF} is the macroscopic ground-state energy from the Thomas-Fermi model of ref. [123]. Both quantities do not contain neither shell nor pairing effects. $E_{gs-nopair}^{exp}$ was taken from the 2012 Atomic Mass Evaluation, averaged over odd-even staggering in Z and N. The quantity $E_{gs-nopair}^{exp} - E_{gs}^{TF}$ defines the empirical ground-state shell correction, represented by δU_{gs} in figure 4.

In accordance with ref. [128], the overall isotopic trend of the empirical barriers is very well reproduced by B_f^{topo}. However, there are some systematic deviations in the absolute values: Firstly, the barriers of thorium, protactinium and uranium isotopes are overestimated, while the barriers of the heaviest elements plutonium, americium and curium are underestimated. The deviation shows a continuous smooth trend as a function of Z. Secondly, a systematic odd-even staggering that is evident in the empirical barriers from protactinium to curium is not reproduced by the B_f^{topo} values estimated with equation 6.

In ref. [124], a very good reproduction of the empirical barriers was obtained by applying a simple Z-dependent correction to the values obtained by equation (6) and by increasing the pairing-gap parameter Δ at the barrier in proton and neutron number to $14/\sqrt{A}$ MeV. These values are also shown in figure 5. Indications for an increased pairing gap at the barrier were already discussed by Bjørnholm and Lynn [130]. They interpreted this finding as a possible evidence for surface pairing.

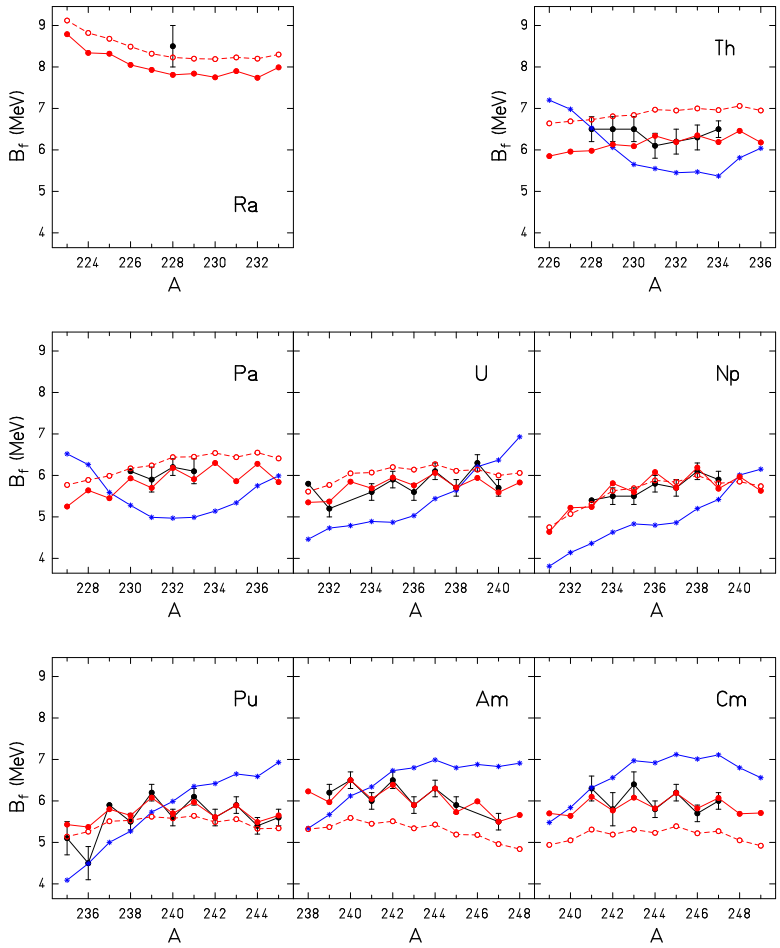

Figure 5: (Color online) The empirical fission threshold of ref. [130] (full black circles) is compared to the value (open red circles) estimated from the topographic theorem according to equation (6) for isotopic sequences of different elements. In addition, a modified estimation (full red circles) with a Z-dependent shift and an assumed increased pairing parameter $\Delta_f = 14/\sqrt{A}$ MeV at the barrier (see text and ref. [124]) as well as the theoretical prediction of the microscopic-macroscopic approach of ref. [131] (blue asterisks) are shown. Empirical values without error bars are given without an uncertainty range in ref. [130]. The figure is taken from ref. [124].

In addition, figure 5 shows the predictions from $Z = 90$ to $Z = 96$ of an elaborate theoretical model [131] with the macroscopic-microscopic approach based on on a meticulous mapping of the potential in five-dimensional deformation space [111]. The model values deviate appreciably from the empirical values. In particular, the isotopic trend is not well reproduced. Moreover, the model does not show the observed odd-even staggering of the barrier height. Other models, macroscopic-microscopic or fully microscopic ones, show similar deviations.

From our study, we may draw the following conclusions:

Considering that (i) the procedure used by Bjørnholm and Lynn for extracting the empirical fission barriers from the measured energy-dependent fission cross sections and probabilities, and (ii) the application of the topographic theorem for obtaining estimated values of the fission barriers are completely independent, the good agreement of these sets of values is a strong indication that, firstly, the empirical barriers deduced by Bjørnholm and Lynn represent the *true* fission thresholds with a remarkable precision and that, secondly, the topographic theorem is a rather good approximation. From the rms deviation between these two sets of barriers, given in table 3, it may be concluded that the uncertainties of the empirical barriers, determined by Bjørnholm and Lynn, are not larger than 500 keV, which is appreciably smaller than the presumed value of 1 MeV mentioned above.

Table 3: Rms deviation between different sets of fission barriers.

	topographic	adjusted	Möller	RIPL 3
empirical	0.52	0.24	1.42	0.36

Note: The table lists the rms deviations in MeV of the different sets of fission barriers shown in figure 5 and the values of RIPL 3 from the empirical values. References: empirical [130], topographic (this work, equation (6)), adjusted (this work and ref. [124]), Möller [131], RIPL 3 [14]. Note that refs. [14] and [131] do not cover all nuclei, for which empirical values are available. The typical uncertainty of the empirical values, given in ref. [130], is 0.2 to 0.3 MeV.

The fact that the deviations can even substantially be reduced by a simple Z-dependent shift indicates that these deviations are caused by systematic shortcomings in the Z dependence of the macroscopic model used for the estimations or by a slight violation of the topographic theorem. By applying the deduced Z-dependent shift and an increased odd-even staggering at the saddle, the empirical barriers are reproduced within their given

uncertainties of 200 to 300 keV. Regarding the absence of any systematic deviations along isotopic chains, it seems that it is well justified to assume that reliable predictions of fission thresholds in an extended region of the chart of the nuclides can be made with this description. The agreement of this parametrization with the empirical values proposed in RIPL 3 is less good (see Figs. 7 and 8 in ref. [122]), in particular in the structures along isotopic chains, which are not affected by the applied Z-dependent shift. This gives more confidence to the empirical values of Bjørnholm and Lynn.

In a more fundamental sense, any noticeable structural effects on the fission-barrier height can be attributed to the microscopic contributions to the ground-state mass and to a systematically stronger odd-even staggering at the barrier, only. Other structural effects in the vicinity of the fission barrier do not exceed the given uncertainties of the empirical fission thresholds that amount to typically 200 keV. An influence of shell effects at the barrier on the barrier height cannot strictly be excluded, but if there is any, it must show a gradual and smooth variation with Z and A. At present, theoretical estimates of the fission barriers do not yet attain this precision. They show deviations in the order of 1 MeV. The best reproduction of empirical fission barriers has been reported in ref. [132], where an rms deviation of 0.5 MeV has been obtained within the framework of the macroscopic-microscopic approach. This is also the precision to be expected for theoretical calculations of the whole potential-energy landscape of the fissioning system.

4.3.2 Hidden regularities of fission channels

Although the good description of the fission barriers by the topographic theorem that is demonstrated in section 4.3.1 means that the saddle mass is essentially a macroscopic quantity, many other fission quantities show very strong signatures of nuclear structure, for example, the evolution of the shape and the potential on the fission path, in particular the existence of fission isomers, triaxiality at the first barrier and mass asymmetry at the second barrier due to shape-dependent shell effects. Also the fission-fragment yields are characterized by several components in the mass distributions from different fission channels that are attributed to shell effects in the potential energy and by an odd-even staggering in proton and neutron number due to the influence of pairing correlations. The potential-energy surface of the ^{238}U nucleus, calculated with the two-center shell model in ref. [125], demonstrates the structures created by the microscopic contributions.

The mass-asymmetric deformation belongs to the relevant degrees of freedom of most dynamical fission models, and the manifestation of shell

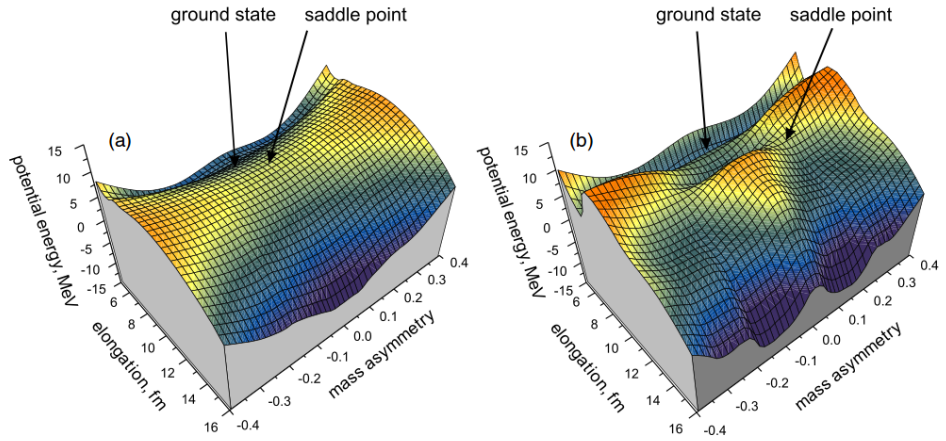

Figure 6: (Color online) Macroscopic (a) and macro-microscopic (b) potential energy surface for the ^{238}U nucleus as a function of elongation and mass asymmetry. The macroscopic part is normalized to zero for the spherical shape of the compound nucleus. See ref. [125] for details. The figure is taken from ref. [125].

effects in the fission-fragment mass distributions plays a prominent role in benchmarking these models. Macroscopic-microscopic models and, to some extent, also fully microscopic self-consistent models were rather successful in reproducing the appearance of mass-asymmetric fission in the actinides, the features of multi-modal fission around ^{258}Fm [133], the gradual transition from single-humped to double-humped distributions around ^{226}Th [115] and, most recently, the appearance of complex mass distributions in a region around $Z \approx 80$ to $Z \approx 83$ from beta stability to the proton drip line [33]. However, the deviations from the measured data remain important, see the examples in figures 2 and 3. A much higher precision has been obtained with the semi-empirical description used in the GEF code [122] by exploiting regularities in the characteristics of the fission channels that are not obvious from microscopic models, because these models treat each fissioning nucleus independently. In the following, we will describe the theoretical considerations that are behind this semi-empirical approach. They are not only important for high-precision estimates of fission yields, but also for a better understanding of the fission process by revealing an astonishingly high degree of regularity in the properties of fission channels.

Early manifestation of fragment shells: When the two-center shell model became available, it was possible to study the single-particle structure in a di-nuclear potential with a necked-in shape. Investigations of Mosel and Schmitt [134] revealed that the single-particle structure in the vicinity of the outer fission barrier already resembles very much the coherent superposition of the single-particle levels in the two separated fragments after fission. The authors explained this result by the general quantum-mechanical feature that wave functions in a slightly necked-in potential are already essentially localized in the two parts of the system. Also recent self-consistent calculations show this feature (e.g. ref. [84, 86]), which is a direct consequence of the necking, independent from a specific shape parametrization. This finding immediately leads to the expectation that the shells on the fission path that are responsible for the complex structure of fission modes are essentially given by the fragment shells. Potential-energy surfaces of fissioning systems calculated with the macroscopic-microscopic approach, for example ref. [131], support this assumption. The fact that in the actinides, for which a double-humped fission-fragment mass distribution is observed, theoretical models predict a mass-asymmetric shape at the outer saddle, suggests also that fragment shells are already established to a great extent at the outer saddle.

As a consequence, the shell effects on the fission path from the vicinity of the second barrier to scission can be approximately considered as the sum of the shell effects in the proton- and neutron-subsystems of the light and the heavy fission fragment. Thus, these shells do not primarily depend on the fissioning system but on the number of neutrons and protons in the two fission fragments. However, these shells may be substantially different from the shell effects of the fragments in their ground state, because the nascent fragments in the fissioning di-nuclear system might be strongly deformed due to their mutual interaction.

Thus, the potential energy can be understood as the sum of a macroscopic contribution, depending on the fissioning nucleus, that changes gradually on the fission path and from one system to another one, and a microscopic contribution that depends essentially only on the number of protons and neutrons in the nascent fragments. Thus, in nuclear fission, the macroscopic-microscopic approach turns out to be particularly powerful. The distinction of the two contributions to the potential is accompanied with an assignment of these contributions to different systems: The macroscopic potential is a property of the total system, while the shell effects are attributed to the two nascent fragments [135]. Figure 7 illustrates, how the interplay of these two contributions can explain why symmetric fission is

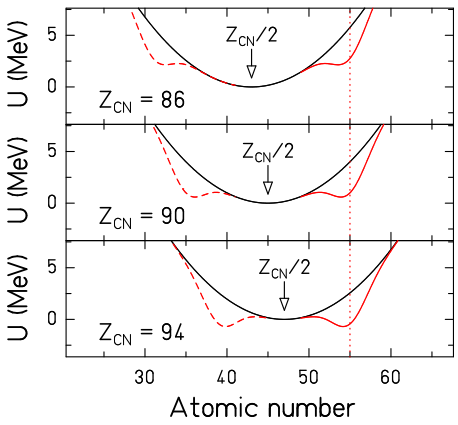

Figure 7: (Color online) Schematic illustration of the potential energy for mass-asymmetric shape distortions on the fission path, after an idea of Itkis et al. [136]. The black curve shows the macroscopic potential that is minimum at symmetry, while the red curve includes the extra binding due to an assumed shell appearing at Z=55 in the heavy fragment. The figure is taken from ref. [122].

energetically favored for fissioning nuclei below thorium, while asymmetric fission is favored for nuclei above thorium. The shell effects used for the three nuclei on figure 7 are the same. The changes in the total potential are caused by the shift to higher Z values of the minimum of the macroscopic potential, which is located at symmetry.

Quantum oscillators of normal modes: The early manifestation of fragment shells provides the explanation for the appearance of fission valleys in theoretical calculations of the potential-energy landscape of fissioning nuclei, in particular in the actinides. As demonstrated in figure 6, these are valleys in direction of elongation, starting in the vicinity of the second barrier until scission, with an almost constant position in mass asymmetry. For the dynamic evolution of the fissioning system, this means that each valley can be considered as a quantum oscillator in the mass-asymmetry degree of freedom. The initial flux in each valley, corresponding to a specific fission channel, is decided at the second barrier. Depending on the height of the ridge between neighboring fission valleys, there might be some exchange of flux further down on the way to scission. The positions of the asymmetric

minima that are created by shell effects and the shape of the corresponding oscillator potentials stay approximately constant until scission, but the excitation energy of each quantum oscillator tends to increase on the way towards scission by the feeding from the potential-energy gain along the fission path. It is assumed that the ensemble averaging of a large number of fission events establishes an excitation-energy distribution that can formally be replaced by the distribution of a quantum oscillator in instantaneous equilibrium with a heat bath of temperature T, whereby the temperature increases on the way to scission. With these ideas in mind, one can formulate the evolution of the mass-asymmetry degree of freedom of the fissioning system on the way to scission. Deviations from instantaneous equilibrium by a dynamical freeze-out will be discussed in the next section.

Since tunneling occurs with a very low probability, as can be deduced from the long spontaneous-fission half lives, an excited nucleus has enough time to re-arrange its available energy before. The probability for the passage of the fission barrier increases considerably, if the nucleus concentrates enough of its energy on the relevant shape degrees of freedom for avoiding tunneling as much as the available energy allows. If the available energy exceeds the barrier, this excess can be randomly distributed between the different states above the barrier without any further restriction, such that the barrier is passed with maximum possible entropy on the average [137], replacing again event averaging by instantaneous equilibrium. For this reason, the fissioning system has no memory on the configurations before the barrier, except the quantities that are preserved due to general conservation laws: total energy, angular momentum and parity. Thus, the starting point for calculating the properties of the fission fragments is the configuration above the outer fission barrier.

The evolution of the entropy plays a decisive role in the fission process. The concentration of a sufficiently large amount of energy into the elongation degree of freedom in order to overcome the fission barrier essentially without tunneling, if the total energy is sufficiently high, induces a reduction of the entropy.[5] Moreover, the levels at the barrier are populated according to their statistical weights. After passing the barrier, the entropy increases again due to dissipation. Therefore, we think that the approximation of treating fission as an isentropic process [139, 140] is not a generally valid

[5]We would like to stress that this reduction of entropy is not in contradiction to the Second Law of Thermodynamics, because the laws of thermodynamics have a statistical nature. Thermodynamical quantities such as the entropy are subject to fluctuations that become sizable in mesoscopic or microscopic systems like nuclei. A proper way to treat such systems is the explicit application of statistical mechanics [138].

assumption.

Beyond the outer barrier, the distribution of the mass-asymmetry coordinate is given by the occupation probability of the states of the quantum oscillators in the respective fission valleys. The situation is schematically illustrated in figure 8 for the mass-asymmetry coordinate in two fission valleys that are well separated, assuming that the potential pockets have parabolic shape. The fission-fragment mass distribution is given by the evolution of the respective collective variable, until the system reaches the scission configuration. It is defined by the number and the energy distribution of occupied states in the different valleys.

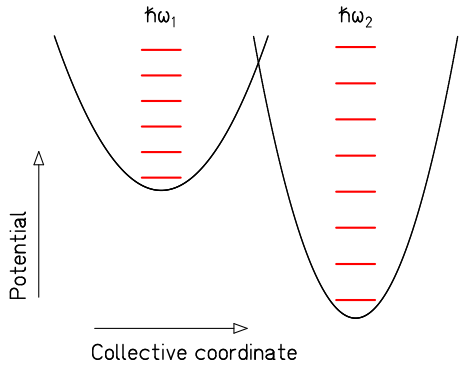

Figure 8: (Color online) Schematic drawing of the potential energy as a function of a collective coordinate that is orthogonal to the fission direction at a fixed elongation. In the present context, the two harmonic oscillator potentials with different depths and $\hbar\omega$ values represent the potential in two fission valleys for mass-asymmetric distortions that are related to different fission channels. The energies of the stationary states are indicated by the red horizontal lines. The overlapping of the two potential-energy curves illustrates the possibility that the fission valleys are divided by a higher ridge that becomes perceptible when a continuous transition from one valley to the other is established in a deformation space with a sufficiently high dimension, see for example ref. [141].

In the case of weak coupling and in thermal equilibrium with a heat bath of temperature T, the ratio of the yields Y_i of the two fission channels corresponding to the population of the two harmonic quantum oscillators depicted in figure 8 is given by

$$Y_2/Y_1 = e^{-\Delta E/T} \cdot \frac{\hbar\omega_1}{\hbar\omega_2} \approx e^{-\Delta E/T}. \quad (7)$$

$\Delta E = E_2 - E_1$ is the potential-energy difference between the bottoms of the two quantum oscillators. As indicated, the relation is strongly dominated by the exponential term. The distribution of the collective coordinate of the quantum oscillator for asymmetric distortions in one fission channel is a Gaussian function with a variance σ^2 that is given by the well known equation

$$\sigma^2 = \frac{\hbar\omega}{2C}\coth(\frac{\hbar\omega}{2T}). \quad (8)$$

C is the second derivative of the potential near its minimum in the direction of mass asymmetry.

If the exchange of flux between different fission channels beyond the second barrier is negligible, the temperature parameter in equation (7) is the value at the second barrier, while the width of mass asymmetric distortions, described by the temperature parameter in equation (8), evolves on the way to scission. The width of the fission-fragment mass distribution is given by the temperature at the dynamical freezout that is described in the following.

Dynamical freeze-out: It is well known [142] that the statistical model, applied to the scission-point configuration, is unable of explaining the variances of the mass and energy distributions and their dependence on the compound-nucleus fissility. Also stochastic [108, 110] and self-consistent models [82] show the importance of dynamic effects on the width of the fission-fragment mass distributions, especially in low-energy fission. Studies of Adeev and Pashkevich [143] suggest that dynamical effects due to the influence of inertia and dissipation can be approximated by considering the properties of the system at an earlier time. That means that the statistical model may give reasonable results if it is applied to a configuration that depends on the typical time constant of the collective coordinate considered. The memory time is specific to the collective degree of freedom considered. It is relatively long for the mass-asymmetric distortions [144] and rather short for the charge-polarization degree of freedom [145, 146, 147, 148]. Thus, the shape of the potential and the value of the respective collective temperature that are decisive for the distribution of the respective observable are those that the system takes at the respective memory time before scission, which can be considered as a kind of freeze-out.

From these considerations, it may be concluded that the observed fission-fragment mass distribution of a specific fission channel can approximately

be understood as the equilibrium distribution of the quantum oscillator in the mass-asymmetry degree of freedom in the corresponding fission valley at the time of freeze-out on the fission path with the local mass-asymmetric potential, temperature, friction, and inertia.

Empirical extraction of universal fragment shells: In the macroscopic-microscopic approach, the potential energies at the bottom of the different fission valleys that determine the relative yields of the fission valleys according to equation (7) are the sum of 5 terms: the macroscopic potential and the shell energies of the proton and neutron subsystems of the two nascent fragments. The stiffness of the macroscopic potential against mass-asymmetric distortions evolves gradually as a function of the fissility [96]. An empirical function has been deduced with a statistical approach [149] from the widths of measured mass distributions of the symmetric fission channel at higher excitation energies, where shell effects are essentially washed out. For describing the yields and the variances of the contribution of each fission channel to the fission-fragment mass distributions with equations (7) and (8), the following 3 parameters are required in addition to the curvature of the macroscopic potential: the position, the magnitude and its second derivative of each shell in each of the four subsystems (protons and neutrons in the light and the heavy pre-fragment). These parameters are expected not to depend on the fissioning system, and to stay constant on the way to scission, once the fragments have acquired their individual properties.

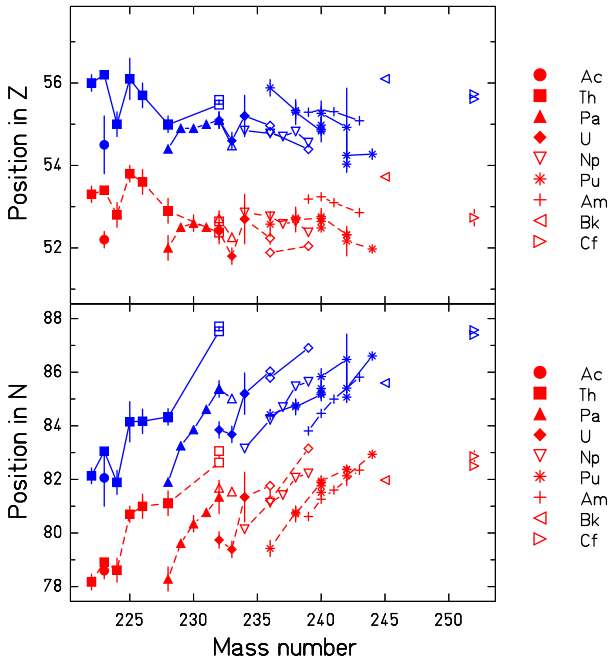

Figure 9: (Color online) Mean positions of the standard fission channels in atomic number (upper part) and neutron number (lower part) deduced from measured fission-fragment mass and element distributions. Values were converted from measured atomic numbers or mass numbers using the unchanged-charge-density assumption and neglecting neutron evaporation. The shape of the symbol denotes the element as given in the legend of the figure. Data from ref. [45] are marked by solid symbols. The values of standard 1 (standard 2) for the isotopes of a given element are connected by dashed (full) lines and marked by red (blue) symbols. The figure is taken from ref. [63].

It is known since long that the mean mass of the *heavy* component in asymmetric fission of the actinides is approximately constant at $A \approx 140$ [150]. This is an indication that shells in the heavy fragment are dominant. Böckstiegel et al. [63] compiled a systematics of fission channels, deduced from measured fission-fragment mass and element distributions, partly from two-dimensional mass-TKE distributions. The systematics of the mean proton and neutron numbers of the standard 1 and the standard 2 fission channels, following the nomenclature of Brosa et al. [23], is shown in figure 9. Obviously, the standard 1 and the standard 2 channels are located at the proton numbers $Z \approx 52$ and $Z \approx 55$, respectively. This feature is most clearly evidenced by the data from the long isotopic chains measured in electromagnetic fission of relativistic secondary beams [45], but it had already been observed for proton-induced fission of isotopic chains of heavier elements by Gorodisskiy et al. [151]. In contrast, the neutron number varies systematically as a function of the mass of the fissioning nucleus.

This means that the most prominent asymmetric fission channels, standard 1 and standard 2, are caused each by a fragment shell that fixes the number of protons in the heavy fragment at $Z \approx 52$ and $Z \approx 55$, respectively. A discussion of this finding in view of the shell model is found in section 5.4.1.

The ideas outlined above with a few refinements were applied for describing with a remarquable precission the fission yields of a great number of fissioning systems ranging from $Z = 80$ to $Z = 112$ in the semi-empirical GEF model using a unique set of parameters [122]. To illustrate the quality of GEF, figure 10 shows calculated fission-fragment mass distributions compared to evaluated data for some selected nuclei. A much more detailed comparison covering a large variety of fission observables for many fissioning systems and different energies can be found in [122].

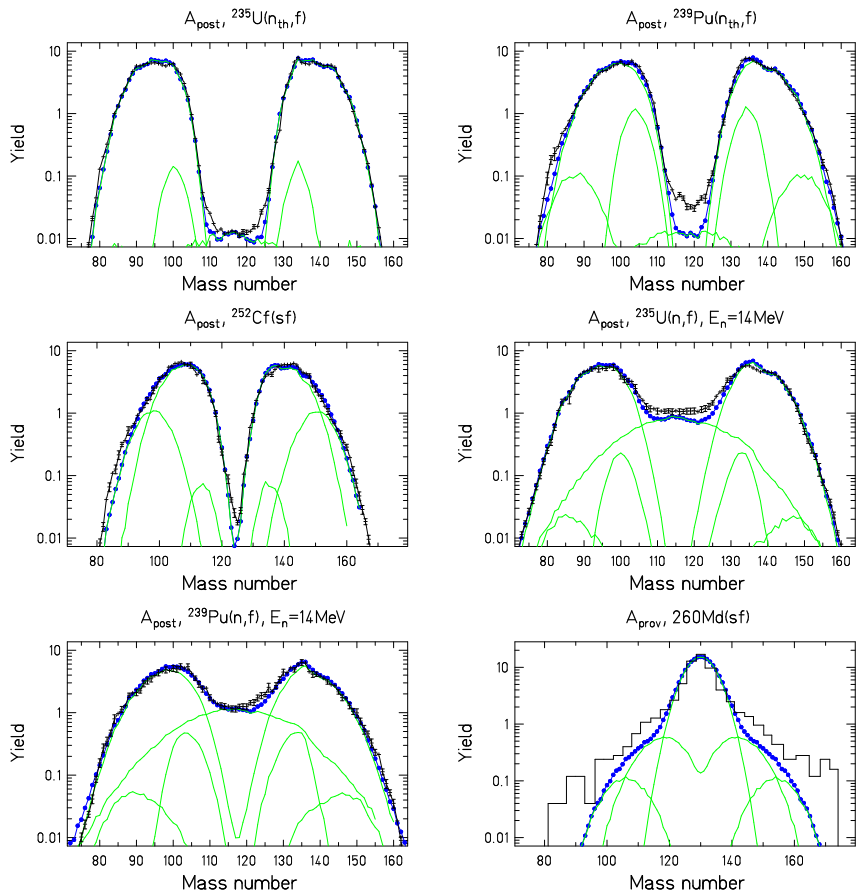

Figure 10: (Color online) Evaluated and measured mass distributions (black symbols) of fission fragments in comparison with the result of the GEF model (blue symbols). The mass distributions after prompt-neutron emission are taken from the evaluation of ref. [152]. The provisional masses from spontaneous fission of ^{260}Md (black histogram) were directly deduced from the ratio of the fragment energies without applying a correction for prompt-neutron emission. They are taken from ref. [21]. The green lines show the calculated contributions from the different fission channels. The figure is taken from ref. [124].

4.3.3 Heat transport between nascent fragments

The transformation of energy between potential energy, intrinsic and collective excitations as well as kinetic energy is a very important aspect of the nuclear-fission process. It determines the partition of the fission Q value (plus eventually the initial excitation energy of the fissioning system) between kinetic and excitation energy of the final fragments. Moreover, the division of the total excitation energy between the fragments is of considerable interest, because it strongly influences the number of prompt neutrons emitted from the fragments. Thus, it also induces a shift towards less neutron-rich isotopes.

Dissipation on the fission path: As mentioned above, the description of dissipation in the fission process, in particular in low-energy fission, where pairing correlations play an important role, still poses severe problems to theory. In the range of pairing correlations that is important in low-energy fission. Bernard et al. [87] developed the Schrödinger Collective Intrinsic Model for describing the coupling between collective and intrinsic two-quasiparticle excitations on the fission path in an extended Hartree-Fock-Bogoliubov approach. Tanimura et al. [86] recently observed deviations from the adiabatic limit of the microscopic transport theory by single-particle levels crossing in the vicinity of the fission barrier. Once the nascent fragments acquire their individual properties, the single-particle levels stay approximately parallel, and the process is essentially adiabatic. Shortly before scission, one-body dissipation becomes stronger due to the fast shape changes connected to the neck rupture.

It is expected that the effects on the fission observables from these two processes are rather different. Because the relaxation time of intrinsic excitations is short compared to the estimated saddle-to scission time[6], one may assume that the induced nucleonic excitations are, on the average, equally distributed over all intrinsic degrees of freedom of the fissioning system when it reaches the scission configuration. The dissipation near scission, however, occurs so shortly before neck rupture that the equilibration of the dissipated energy may be expected to happen to a great part after scission, where exchange between the fragments is inhibited.f

The dissipated energy is fed by the potential-energy difference between

[6]The characteristic time for the thermalization of the intrinsic excitation energy of a nucleus is a few times the time a nucleon needs to travel over the diameter of the nucleus with the Fermi velocity. This is in the order of a few times 10^{-22} s. The estimated saddle-to-scission time is appreciably longer, about 10^{-20} s [95] or even longer [79].

outer barrier and scission for which Asghar and Hasse derived a general estimation [153]. This energy difference gives an upper limit of the dissipated energy, because it is shared by intrinsic excitations, collective excitations and pre-scission kinetic energy.

Statistical properties of the nascent fragments: As already mentioned, we assume that the intrinsic excitation energy, consisting of the intrinsic excitation energy above the outer barrier plus the energy dissipated in the region of strong level crossing behind the barrier is, averaged over many fission events, equally distributed over all intrinsic degrees of freedom of the fissioning system when it reaches scission. The division of this excitation energy E_{tot} among the nascent fragments in statistical equilibrium is determined by the number of states available in the two nuclei. Thus, the distribution of excitation energy E_1 of one fragment before neck rupture is calculated by the statistical weight of the states with a certain division of excitation energy between the fragments

$$\frac{dN}{dE_1} \propto \rho_1(E_1) \cdot \rho_2(E_{tot} - E_1). \tag{9}$$

Note that ρ_1 and ρ_2 are the level densities of the fragments in their shape just before scission, not in their ground-state shape! The remaining energy $E_{tot} - E_1$ is taken by the other fragment.

There exist several analytical level-density descriptions, e.g. refs. [154, 155, 161, 14, 157], and, recently, also a few microscopic calculations [158, 159, 160]. In the present context, we are not interested in describing the peculiarities of specific systems, but to understand the main thermodynamical properties of a nucleus that determine the average behavior of the energy division between the nascent fragments. For this purpose, using a global level-density description is better suited and more transparent than using individual results of microscopic models for specific nuclei. General investigations of the validity of recommended parametrizations can be found in refs. [161, 162, 14]. These were rather oriented in benchmarking the level-density descriptions against empirical data derived from level counting, neutron resonances and evaporation spectra. However, in ref. [163] it was pointed out that many level-density descriptions violate basic theoretical requirements, in particular in the low-energy range where pairing correlations play an important role. These violations are often not easily recognized or checked by a comparison with experimental data due to their incompleteness and uncertainty, but they can be important in view of the dynamic nuclear properties in terms of statistical mechanics.

The requirements, formulated in [163], are:

- The level density below the critical pairing energy, the excitation energy where pairing correlations disappear[7], is characterized by an approximately exponential function, corresponding to a constant temperature. This is qualitatively explained by the phase transition from super-fluidity to a Fermi gas that stores any additional energy in creating additional degrees of freedom by quasi-particle excitations instead of an increasing temperature. In addition to the empirical evidence, for example from experiments performed at the Oslo Cyclotron Laboratory [165], a theoretical justification on the basis of the BCS approximation was given recently by Moretto et al. [166], where the thermodynamical nuclear properties are considered as a function of excitation energy instead of the temperature as usually done before, e.g. [164]. Empirical constant-temperature parametrizations, e.g. ref. [157] or ref. [167], represent the level density in this energy range rather well.

- The level densities of neighboring even-even, odd-mass and odd-odd nuclei are essentially identical, except the gradual systematic dependence on the mass and the variation of the shell effect, when the energy scale is shifted to exactly eliminate the odd-even staggering of the binding energies. The main differences are the additional levels below the pairing energy Δ or two times Δ in odd-mass and even-even nuclei, respectively, if compared to odd-odd nuclei. This feature has already been described by Strutinsky [168] with an analytical solution of the pairing problem in a Boltzmann gas. (See also figure 9 of ref. [64].) It is stressed again in ref. [166]. As can be seen in figure 11, the experimental level densities obtained with the Oslo method fulfil fairly well this requirement: The level densities of neighboring nuclei converge when the excitation energy is shifted accordingly.

- The level density above the critical pairing energy is well represented by the Bethe formula of independent fermions [169], which is also known as the Fermi-gas level density, with an energy shift by the pairing condensation energy with respect to the ground state. This energy shift includes an odd-even staggering that eliminates the odd-even staggering of the nuclear binding energy (see previous point). In addition, the collective enhancement is considered by the application of an appropriate factor. Shell effects can additionally be taken into account, for example by the analytical formula of Ignatyuk et al. [155].

[7] Strictly speaking, this transition is not sharp due to the small size of the nucleus [164].

The resulting level-density description, proposed in ref. [163] resembles the composite level-density formula of Gilbert and Cameron [154], however with an increased matching energy in the order of 10 MeV. This value of the matching energy, which can also be interpreted as the critical pairing energy, is in good agreement with results of an analysis of measured angular distributions of fission fragments [170] and energy-dependent fission probabilties [155].

Energy sorting: From the previous discussion, we conclude that a fissioning nucleus on the way to scission develops from a mononucleus to a dinuclear system, where two nascent fragments acquire their individual thermodynamical properties well before scission. Because they are still connected by a neck, they can exchange nucleons and excitation energy [171]. At moderate excitation energies, the two nascent fragments form a rather peculiar system: They act like microscopic thermostates. Each fragment can be considered as a heat bath for the other fragment, although the system has a rather small fixed number of particles and a rather low fixed amount of total energy. Disregarding shell effects, the nuclear temperature in the constant-temperature regime decreases systematically with the fragment mass: $T \propto A^{-2/3}$ [157].

Figure 11 illustrates the variation of the logarithmic slope of the level density of the fission fragments as a function of mass in the reduced energy scale. This proves that the light fragment has a systematically higher temperature than the heavy one. The influence of shell effects may inverse this tendency only in nearly symmetric splits.

As a consequence, the intrinsic energy (heat) tends to flow to the heavier nascent fragment that has the lower temperature. This process of energy sorting has first been described in ref. [7]. The process of heat exchange is subject to large fluctuations that allow the application of thermodynamical concepts [171]. With increasing initial excitation energy, the fragments enter the Fermi-gas domain, and the energy sorting gradually disappears [172]. Asymptotically, at high excitation energy, the heat is shared by the fragments in proportion to their masses.

Prompt-neutron yields: There are several observables that provide information on the energetics of the fission process. These are the total kinetic energy of the fragments, and the energy spectra and multiplicities of prompt neutrons and prompt gammas. Among those, the prompt-neutron multiplicity gives the most direct and the most detailed information, because it can

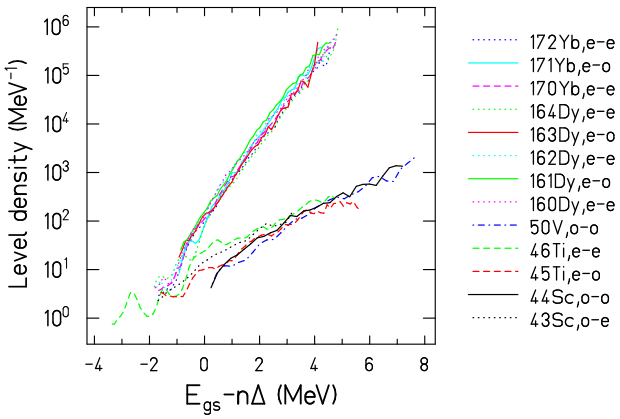

Figure 11: (Color online) Experimental level densities of various nuclei in a reduced excitation-energy scale $U = E_{gs} - n \cdot \Delta(\Delta = 12/\sqrt{A})$. The excitation energy above the ground state E_{gs} is reduced by $2 \cdot \Delta$ ($n = 2$) for even-even (e-e) nuclei, by Δ ($n = 1$) for even-odd (e-o) or odd-even (o-e) nuclei and left unchanged ($n = 0$) for odd-odd (o-o) nuclei. The figure is taken from ref. [182], where also the references of the data can be found.

individually be attributed to a specific fragment. Moreover, neutron evaporation is by far the most probable decay channel when the excitation energy exceeds the neutron binding energy. Thus, the excitation energy of a specific fragment is given to a good approximation by the sum of the neutron binding energies and the mean neutron kinetic energies that, which can be estimated rather reliably, plus an offset of about half the neutron binding energy of the final fission product that ends up in prompt-gamma emission, if the angular momentum of the fissioning nucleus is not too high.

More than 40 years ago, the measurement of prompt-neutron multiplicities was a subject of great interest, see for example [173, 174, 175, 176, 177]. Several experiments were performed to determine the mass-dependent average neutron multiplicity as a function of the initial excitation energy of the fissioning system. Figure 12 shows an evaluation of this kind of data for neutron- and proton-induced fission of ^{238}U for different energies of the incoming particle from Wahl [178]. It should be noted that the observed events from proton-induced fission sum up from different fission chances. That means that the excitation-energy distribution at the saddle deforma-

tion reaches from the initial excitation energy down to energies in the vicinity of the fission barrier.

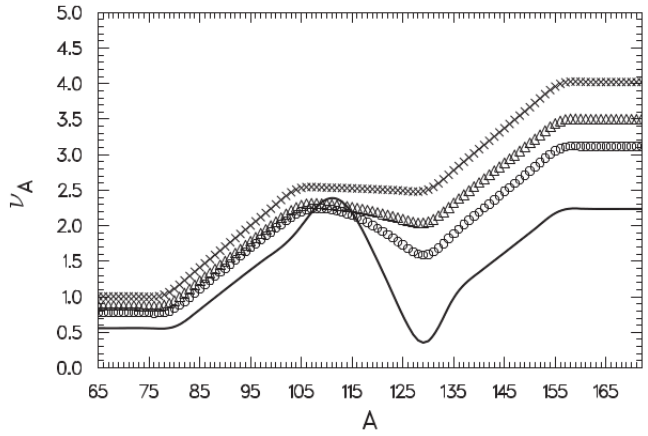

Figure 12: Evaluation of measured prompt-neutron multiplicities as a function of fragment mass for proton- and neutron-induced fission of ^{238}U [178]. Explanation of symbols: ^{238}U + p, o = 30 MeV, $\triangle$ = 50 MeV, $\times$ = 85 MeV; line = ^{238}U(n$_{fast}$,f). The figure is taken from ref. [178].

The curve for the fast-neutron-induced fission of ^{238}U in figure 12 shows a saw-tooth behavior that is typical for the prompt-neutron multiplicities in the actinides. An explanation in terms of fragment shells that determine the deformation of the fragments at scission was given by Wilkins et al. in their scission-point model [26]: As a result of their shell-model calculations, the energetically favorable deformation of the light and the heavy fragments increases with the mass of the fragment. This deformation energy is thermalized after fission and feeds the evaporation of neutrons. The minimum around $A = 130$ is attributed to fragments near the doubly magic spherical ^{132}Sn. Another salient feature of these data is that almost all additional energy induced by an increasing incoming-particle energy ends up in the heavy fragment. This feature remained unexplained, in spite of many attempts. The discovery of energy sorting provides a convincing explanation for the transport of essentially all additional excitation energy that is brought into the system to the heavy fragment. Previous model calculations could not reproduce these data, because the division of excitation energy at scission was estimated on the basis of the Fermi-gas level density. The particularities at energies below the critical pairing energy due to pairing correlations

where not considered.

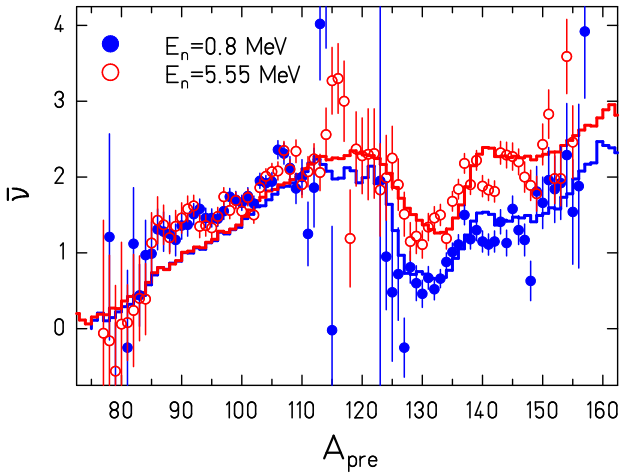

Figure 13: (Color online) Measured prompt-neutron multiplicity in ^{237}Np(n,f) as a function of pre-neutron mass at two different incident-neutron energies [180] (data points) in comparison with the result of the GEF model [122] (histograms). The figure is taken from ref. [120].

The quantitative estimation of the mass-dependent prompt-neutron multiplicities in proton-induced fission is complicated by the contributions from multi-chance fission. Rather precise experiments on mass-dependent prompt-neutron multiplicities below the threshold for second-chance fission were performed by Müller et al. [179] and Naqvi et al. [180] with incident neutrons of different energies. The data of ref. [180] are compared in figure 13 with a calculation performed with the GEF code that considers the constant-temperature behavior of the level density in the range of pairing correlations [163]. Due to energy sorting, the prompt-neutron multiplicity in the light fission-fragment group remains the same, in spite of an increase of the initial energy by almost 5 MeV.

We conclude that the application of statistical mechanics is an efficient way to handle the division of excitation energy between the nascent fragments on the fission path. The results reproduce the experimental data on energy sorting with a good precision. Unfortunately, high-quality data of this type are still scarce.

Odd-even effect in fission-fragment yields: The odd-even effect in fission-fragment distributions, both in the number of protons and in the number of neutrons, is one of the most prominent manifestations of nuclear structure. This phenomenon can be studied in analogy to the energy sorting, described above. Also with respect to pairing correlations, the individual fragment properties are assumed to be established well before scission [181], and statistical equilibrium before scission may be assumed.

As already mentioned in a previous section, the nuclear level densities considered on an absolute energy scale evolve smoothly without any noticeable odd-even staggering as a function of the number of protons and neutrons, except the appearance of additional levels compared to odd-odd nuclei, with a fully paired configuration in even-even nuclei and with fully paired configurations in the proton respectively neutron subsystem in odd-A nuclei, see figure 11. Therefore, the appearance of odd-even staggering in fission yields must be connected in some way with these fully paired configurations. Indeed, at reduced energies above the ground-state level of odd-odd nuclei, the statistical weight of excited states is equal in all classes of nuclei (even-even, even-odd, odd-even and odd-odd), if the smooth mass dependence is neglected. Also the number of available states in even-odd and odd-even nuclei above the level of odd-A nuclei is the same. That means that the overproduction of fragments with even number of protons can be traced back to even-even nuclei that are formed fully paired at scission when statistical equilibrium is assumed.

The odd-even effect in fission-fragment proton or neutron number before neck rupture can quantitatively be calculated by the statistical weight of configurations with even and odd numbers of protons, respectively neutrons, in the nascent fragments.

A schematic model following these ideas has been developed in ref. [182]. See also ref. [122] for the implementation in the GEF code. For an even-even fissioning nucleus, the number of configurations with Z_1 even at fixed total reduced energy U_{tot} is given by:

$$N^{ee}_{Z_1=e}(Z_1) = \int_{-2\Delta_1}^{U_{tot}+2\Delta_2} \rho_1(U_1)_{(ee)}\rho_2(U_{tot}-U_1)_{(ee)}dU_1 + \tag{10}$$

$$\int_{-\Delta_1}^{U_{tot}+\Delta_2} \rho_1(U_1)_{(eo)}\rho_2(U_{tot}-U_1)_{(eo)}dU_1$$

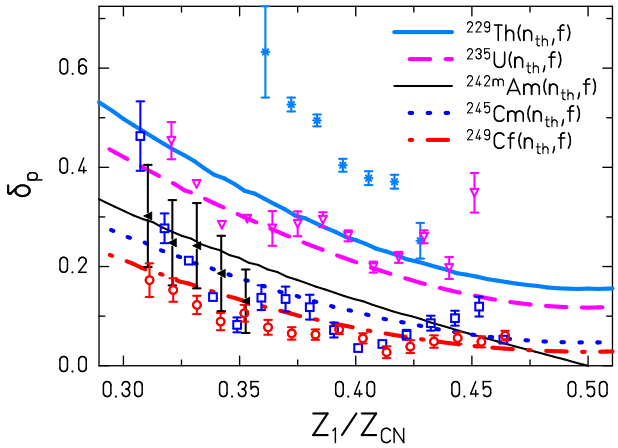

Figure 14: Local logarithmic four-point difference δ_p of the fission-fragment Z distributions as a function of asymmetry, represented by the ratio of the nuclear charge of the light fragment Z_1 and the nuclear charge of the fissioning nucleus Z_{CN}. The symbols show experimental data from the compilation of ref. [65] and denote the target nuclei: ^{229}Th (stars), ^{235}U (open triangles), ^{242}Am (full triangles), ^{245}Cm (open squares), ^{249}Cf (open circles). The lines correspond to the results of the model of ref. [182] described in the text. The figure is taken from ref. [182].

where $\rho_i(U_i)_{(ee)}$ and $\rho_i(U_i)_{(eo)}$ are the level densities of representative even-even and even-odd fragments, respectively, with mass close to A_1 or A_2. The reduced energy U is shifted with respect to the total excitation energy E available in the two nascent fragments $U = E - n\Delta$, $n = 0, 1, 2$ for odd-odd, odd-mass, and even-even fragments, respectively. This ensures the use of a common energy scale in the frame of the fissioning system, which is a basic requirement for the application of statistical mechanics. Long-range variations of the available excitation energy E as a function of mass asymmetry [183] are neglected in the schematic model presented here. They might be additionally considered in a more refined model.

The number of configurations with Z_1 odd for an even-even fissioning

nucleus is:

$$N^{ee}_{Z_1=o}(Z_1) = \int_{-\Delta_1}^{U_{tot}+\Delta_2} \rho_1(U_1)_{(oe)}\rho_2(U_{tot}-U_1)_{(oe)}dU_1 + \tag{11}$$

$$\int_{0}^{U_{tot}} \rho_1(U_1)_{(oo)}\rho_2(U_{tot}-U_1)_{(oo)}dU_1$$

where $\rho_i(U_i)_{(oe)}$ and $\rho_i(U_i)_{(oo)}$ are the level densities of representative odd-even and odd-odd nuclei, respectively, with mass close to A_1 or A_2. The yield for even-Z_1 nuclei is $Y^{ee}_{Z_1=e}(Z_1) = N^{ee}_{Z_1=e}(Z_1)/N^{ee}_{tot}(Z_1)$ with $N^{ee}_{tot}(Z_1) = N^{ee}_{Z_1=e}(Z_1) + N^{ee}_{Z_1=o}(Z_1)$. Similar equations hold for odd-even, even-odd and odd-odd fissioning systems. The total available reduced intrinsic excitation energy U_{tot} is assumed to be a fraction of the potential-energy difference from saddle to scission plus the initial excitation energy above the barrier [153]. Thus, it also increases with the Coulomb parameter $Z^2/A^{1/3}$ of the fissioning nucleus.

The result of these considerations is that the odd-even effect in fission-fragment Z distributions is caused by the statistical weight of configurations with a concentration of all intrinsic excitation energy and unpaired nucleons in the heavy fragment and the formation of a fully paired light fragment.

This approach reproduces the observed salient features of the proton odd-even effect [65]: (i) The odd-even effect decreases with the Coulomb parameter and with increasing initial excitation energy. (ii) The local odd-even effect, represented by the logarithmic four-point differences, $\delta_p(Z{+}3/2) = 1/8(-1)^{Z+1}(\ln Y(Z{+}3) - \ln Y(Z) - 3[\ln Y(Z{+}2) - \ln Y(Z{+}1)])$, increases towards mass asymmetry. (iii) The local odd-even effect for odd-Z fissioning nuclei is zero at mass symmetry and approaches the value of even-Z nuclei for large mass asymmetry. As shown in figure 14, the quantitative reproduction is satisfactory, except for the system ^{229}Th(n_{th},f). The disagreement found for this system may be caused by the neglect of fluctuations in the dissipated energy. In fact, for a great part of the fission events the available energy of this system may be so low that they reach the scission point in a completely paired configuration due to the threshold character of the first quasi-particle excitation.

It is expected that the same ideas are valid for the odd-even effect in fission-fragment N distributions at scission, that means before the emission of prompt neutrons. However, in the measured number of neutrons

in post-neutron fission fragments this initial odd-even effect is masked by the influence of structural effects in the neutron binding energies on the neutron-evaporation process [184, 185, 186]. This idea explains, why the measured values of δ_N for electromagnetic and neutron-induced fission are very similar, see figure 1. It was successfully implemented in the SPACS code for calculating the nuclide yields of spallation residues [187].

We would like to stress that the model of ref. [182] does not include the effect of the neck rupture. By many authors (see ref. [17]), it is advocated that any production of odd-Z fragments starting from fully paired configurations at saddle is exclusively caused by pair breaking during the fast shape changes connected with the rupture of the neck. However, no quantitative estimation has been presented. This would imply that the motion from saddle to the configuration before neck rupture is totally adiabatic and that a sizable fraction of the unpaired nucleons emerging from the quasiparticle excitations at neck rupture end up in different fragments. These assumptions can only be verified by elaborate microscopic models. The result of Tanimura et al. [86] from TD-EDF theory seems to contradict the first assumption, because they obtained a sizable amount of dissipation before scission in the region of many level crossings in the vicinity of the second barrier. The second assumption is not obvious neither to us, because we expect that the localization of the wave functions in the dinuclear regime, discussed before, also leads to a localization of the pairing correlations in the two nascent fragments. The later transfer of single nucleons from one nascent fragment to the other one might be improbable during the short duration of the scission process. Finding a valid answer to these questions is an important task for dynamical quantum-mechanical models. In any case, the complete energy sorting of the available intrinsic excitation energy, consisting of the initial excitation energy of the system above the outer fission barrier and the dissipated energy, and its effect on the enhanced presence of an even number of protons and neutrons in the light pre-fragment describes well the situation of the system before neck rupture.

The odd-even effect in fission-fragment Z distributions is one of the complex features of nuclear fission that can only be fully understood by dynamical quantum-mechanical models. These models need to be further developed in simultaneously handling dissipation, thermodynamics and quantum localization in a realistic way. At present, the application of statistical models [182] and considerations on the influence of dynamical processes at scission [17] give an idea about the processes that are involved in the problem and that should be further studied.

5 Discussion and outlook

After the detailed report on the different activities in fission research, we will try to give an assessment on the status and the most important achievements that have promoted the understanding of nuclear fission during the last years. This will lead to an outlook on the developments to be expected in the near future and on the challenges to be tackled.

5.1 Status of microscopic theories

There is no doubt that microscopic theories are indispensable for a deeper understanding of the fission process. But in spite of considerable progress and many important results, the theoretical description of the fission process with dynamical microscopic models is still very difficult, because the most advanced models in nuclear physics that have been developed for stationary states are not readily applicable to the decay of a meta-stable state. Intense efforts are presently made to develop suitable theoretical tools. Another difficulty arises from technical limitations. Still, the application of the most advanced models that are based on classical stochastic or self-consistent quantum-mechanical methods is heavily restricted by their high demand on computer resources. In this section, we list some of the most important conceptional and technical challenges to which these theories are confronted.

5.1.1 Restrictions by limited computer resources

Number of relevant degrees of freedom: For both fully microscopic quantum-mechanical and classical stochastic models, the number of relevant degrees of freedom that are presently explicitly treated is insufficient for a realistic calculation of the fission process and for covering the full variety of fission observables. In both families of models, the number of relevant degrees of freedom is presently limited to four or five in the most advanced approaches. The success of the random-walk approach of Randrup, Möller et al. in a five-dimensional deformation space in reproducing the mass distributions of a great number of fissioning systems seems to indicate that the number of relevant degrees of freedom is important for obtaining realistic fission-fragment distributions. Their model is the only one that allows for fully independent shapes of the two nascent fragments. This elaborate feature seems to be more important than the restrictions to a comparably simple handling of the dynamics, assuming overdamped motion and using Metropolis sampling, as long as quantitative results on the energetics of the

fission process, in particular on dissipative phenomena, are not concerned. Progress is expected to come gradually by the continuous development of computer technology.

Neglect or approximate treatment of effects beyond mean field: Another class of difficulties arises from effects beyond mean field in fully microscopic quantum-mechanical models. Explicit handling of the direct interactions between the nucleons (many-body interactions) is very difficult, and, thus, there is put much effort in developing suitable approximate algorithms that do not demand too much computer resources. Questions, how well the physics is still represented, must be answered.

5.1.2 Problems in determining the potential-energy surface

For both the self-consistent microscopic approaches and for the stochastic models, the calculated potential energy in the space defined by the relevant degrees of freedom is the basis for the dynamical calculation. There are several difficulties associated with the determination of this multi-dimensional potential-energy surface.

When a shape parametrization is used, only a restricted class of shapes can be realized. This means that the calculated potential energy is an upper limit of the optimum potential that the nucleus could adopt. The deviations could be reduced by increasing the dimension of the deformation space. However, as said before, the tractable number of relevant degrees of freedom, in particular in a dynamical calculation, is restricted due to the limited computing resources as seen in section 5.1.1.

When the potential energy is determined self-consistently with constraints on some degrees of freedom, this is a safe method to find the optimum shape. However, the optimum shape is determined independently on the different grid points defined by the constraints. This can lead to discontinuities in the shape evolution from one grid point to the next one, because one or several of the degrees of freedom that do not belong to the ones explicitly considered may take very different values. This means that the "real" nuclear potential may have a ridge that is not visible in the calculation [188]. Again here, a small number of dimensions aggravates the problem.

A similar problem arises when in the case of a shape parametrization an optimization with respect to additional shape degrees of freedom is performed individually on each grid point that do not belong to the degrees of freedom explicitly considered in the dynamic calculation [141].

It is important to control the effect of such problems on the result of the dynamical calculation, if they cannot be avoided. The appearance of such problems can be detected by local unphysical fluctuations [188] in the calculated potential-energy landscape. I can be reduced by increasing the number of relevant shape parameters.

As already mentioned in section 4.1, this problem does not exist in the TDSLDA approach [79].

5.2 Aspects of statistical mechanics

Most of the models applied to nuclear fission consider aspects of statistical mechanics only by global properties of the degrees of freedom that are treated as an environment. This is, firstly, the level density of the fissioning system and, secondly, dissipation by the coupling between the relevant degrees of freedom and the environment. Phenomena that are connected with the energy transfer between subsystems of the environment as described in section 4.3.3 are most often not considered.

At present, stochastic models are able to treat dissipation by global descriptions of one-body and two-body mechanisms and to include the effects of pairing correlations and shell effects on the level density for determining the heat capacity of the environment and for deriving the driving force of the fission dynamics.

Self-consistent quantum-mechanical models overcame the restriction to adiabaticity only recently and started to develop methods that enable considering quasi-particle excitations on the fission path [87] and one-body dissipation by the fast shape changes at neck rupture [84].

Energy exchange between the nascent fragments [7] or even the competition between quasi-particle excitations in the neutron and proton subsystems [189] of the fragments were only considered in dedicated approaches. However, for an understanding of the division of excitation energy between the fragments or the odd-even effect in fission-fragment nuclide distributions, the explicit consideration of the two environments in the two nascent fragments and their interaction is indispensable.

Preliminary results about these rather complex features of statistical mechanics with simplifying assumptions were already obtained. These concern the phenomenon of energy sorting [7] and global features of the odd-even staggering in fission-fragment Z distributions [182].

The division of excitation energy between the fragments has recently attracted quite some attention. The energy dissipated separately in the individual nascent fragments on the fission path was estimated by Mirea [190]

and compared with the experimental data. The division of excitation energy between the fragments induced at neck rupture was studied in the sudden approximation [191]. An interesting attempt to study the energy partition between the fragments with a microscopic self-consistent approach has been performed in ref. [88] by considering spatially localized quasi-particles in a frozen scission configuration. The dominant role of statistical mechanics, and particularly the assumption of statistical equilibrium in the division of heat between the nascent fragments before scission that is made in refs. [7, 122], is questioned [88] or criticized [79] by several authors, but the transport of intrinsic excitation energy between the nascent fragments has not yet been explicitly studied with these approaches. In particular, the remarkable experimental result of ref. [180] that an increased initial excitation energy of the fissioning system is found in the heavy fragment, while the neutron multiplicity of the light fragment stays unchanged, has not yet been addressed by microscopic models. This is also true for the complex features of the odd-even effect in fission-fragment Z distributions, which is also described in the framework of statistical mechanics in ref. [182].

5.3 Systematics and regularities

In section 4.3 we presented several combinations of empirical observations and powerful theoretical ideas. They go well beyond purely empirical descriptions, because they do not only reproduce experimental data with a high precision, but, due to their theoretical basis and the small number of adjustable parameters that describe all systems with identical values, they are also expected to provide reliable predictions for a large variety of fission quantities for a wide range of nuclei for which no experimental data exist. The GEF model code [122] that exploits these ideas pursues the tradition of former inventive ideas like the macroscopic-microscopic model [192] and the concept of fission channels [23] and, partly, makes directly use of those.

The relationship between GEF and microscopic fission models may best be illustrated by recalling the role of the liquid-drop model in the development of nuclear mass models, although the dynamical fission process is much more complex than the static properties of a nucleus in its ground state. For a long time, purely microscopic models were not able to attain the precision of the liquid-drop model in reproducing the macroscopic nuclear properties. Only very recently, the precision of fully microscopic and self-consistent models became comparable with the precision of macroscopic-microscopic models [193, 194]. While the powerful basic relations of the liquid-drop model follow directly from the theoretical assumption of a leptodermous

system, the parameter values were determined by an adjustment to experimental masses and other nuclear properties. Only microscopic models were able to relate the values of these model parameters to the properties of the nuclear force [195]. Remembering this analogy clarifies that GEF is not intended to compete with microscopic models, although it is presently better suited as far as the use for applications is concerned. On the contrary, both approaches may be considered to be complementary for extracting physics. In particular, the semi-empirical GEF model helps to uncover regularities that are not directly evident from the fission observables and to recognize the physics content of some systematic trends in the data.

5.4 Uncomprehended observations

Beyond the general inability of theory in explaining many facets of the nuclear-fission process, there are some specific observations that seem to contradict well established knowledge. In the following, we will present one of those cases that we believe to be among the most striking ones.

5.4.1 Dominance of "magic" proton numbers in fission-fragment distributions

The success in reproducing the fission-fragment mass distributions from the fission of actinides by a statistical approach, assuming universal fragment shells superimposed on the macroscopic potential, is already a remarkable result. Even more striking is the constancy of the mean number of protons in the heavy fragment of the contributions from the asymmetric fission channels standard 1 and standard 2 over all systems investigated until now [63]. In particular for the standard 2 fission channel, this finding seems to be in contradiction to the results of shell-model calculations performed by Wilkins, Steinberg and Chasman [26] who attributed this dominant asymmetric fission channel in the actinides to a shell at large deformation in the neutron subsystem at $N = 88$. The deformation of about $\beta = 0.6$ that they found in their calculations is consistent with the neutron multiplicity observed in the heavy fragment. These calculations did not provide any evidence for a proton shell at $Z = 55$ that one might suspect to be responsible for the fixed mean number of protons found in the experiment. Other systematic shell-model calculations performed by Ragnarson and Sheline [196] yielded similar results.

At present, Randrup, Möller et al. [115, 33] performed the most extended systematic calculations of the fission-fragment mass distributions for

a large number of fissioning systems with the Brownian Metropolis shape-motion treatment. It would be very interesting to check in detail, whether the observed constancy of the number of protons in the heavy fragment is reproduced by this and also by other models.

One might imagine a number of reasons for the observation of a constant number of protons in the heavy fragment of the asymmetric fission channels. Some possible explanations could be (i) that the relation between the size of a shell-stabilized pre-fragment and the size of the final fragment is not so strict, for example by a variable division of the number of nucleons in the neck at scission, or (ii) that the shell-model calculations are not realistic and miss a proton shell near $Z = 55$ at large deformation, or (iii) that the assumption of the dominant influence of fragment shells on the position of the fission valleys in mass asymmetry is not valid. In this context, we would like to remind the observation of a mutual support of magicities in the surrounding of spherical doubly-magic nuclei [197]. A similar effect in deformed nuclei may be expected. May be, the interactions between the neutrons and the protons do not permit to consider the shell effects in the neutron and the proton subsystem separately, as this is done in the Strutinsky procedure [198]. However, this would be in contradiction to the observation of a local stabilization by neutron shells at $N = 152$ and $N = 162$ over several elements.

In any case, the constant number of protons in the heavy fragment, found in the contribution of the most important asymmetric fission channels in the actinides, is a very intriguing observation that asks for a deeper understanding.

5.5 Expected progress in the modeling of fission

5.5.1 Extending the relevant degrees of freedom

With the progress in computer technology, the corresponding restrictions will gradually become less severe. First of all, this will allow extending the number of relevant degrees of freedom in stochastic and fully microscopic quantum-mechanical models. For example, it will become customary that the shapes of the two nascent fragments are allowed to develop independently, and the charge polarization will routinely be considered. These developments are important for handling fission-fragment distributions in a more realistic way and fully specified in mass and atomic number [199].

Moreover, the processes responsible for the generation of angular momentum of the fission fragments and the problem of orbital angular momentum

[200] as well as the evolution of the projection of the total angular momentum onto the symmetry axis of the fissioning nucleus [201] and the excitation of other collective modes that are already subject of dedicated theoretical considerations and some stochastic calculations may be performed by microscopic models.

There are strong arguments that the intrinsic and the collective degrees of freedom of the environment form separate thermodynamical units with different temperatures [25, 79]. Forthermore, it appears to be mandatory for describing the heat transport between the nascent fragments that the part of the environment, which comprises the intrinsic degrees of freedom, is divided into two parts, belonging to one and the other fragment. The properties of these partial environments and their interaction should be treated separately.

5.5.2 Effects beyond mean field

More powerful computing resources may also allow to apply more realistic treatments of effects beyond mean field than those that are manageable at present, see section 4.1.

5.5.3 Dissipation

While dissipation, the coupling between the relevant degrees of freedom and the environment, is an inherent part of stochastic approaches, fully microscopic quantum-mechanical models are originally restricted to adiabatic processes. Algorithms for considering dissipative processes are presently being developed, for example by explicitly including the first quasi-particle excitations [87] or by representing the heat bath of stochastic models by a large number of identical quantum oscillators [202]. There is great interest to develop more realistic and more complete representations of the environment that better reflect the complex nuclear properties.

5.5.4 Evolution from the mononuclear to the dinuclear regime

The gradual transition from the mononuclear to the dinuclear regime of two nascent fragments that are coupled by the neck manifests itself in several ways: The early predominance of fragment shells seems to be well established, but also the localization of quasi-particles in the two fragments [181] and the increase of the congruence energy [203] need to be better understood. For example, the odd-even staggering of the fission barrier demonstrated in

section 4.3.1 that is a sign for the shape dependence of the pairing gap is not correctly reproduced by theoretical models, e.g. [131].

5.5.5 Neck rupture

The realistic modeling of the violent processes around scission is very demanding for the treatment of collective dynamics and the induced intrinsic and collective excitations. Progress in self-consistent modeling of quantum localization and other processes around neck rupture is expected to improve the understanding of the instabilities at neck rupture and their effect on different observables like the odd-even effect in fission-fragment Z distributions and in the kinetic energies or the angular momenta of the fission fragments.

5.5.6 Combination of different approaches

Progress in the modeling of nuclear fission may also evolve from exploiting the strengths of methods from different approaches. For example, elaborate stochastic models provide the technical tools for handling dissipation, which is directly considered in the Langevin equations by the friction tensor and the fluctuating term. Even more, the driving force TdS/dq is essentially determined by the derivative of the entropy, a quantity that is primarily a property of the environment. It was mentioned that the explicit inclusion of the intrinsic degrees of freedom in a quantum-mechanical approach is not possible. But without considering in some way the environment that creates driving force, friction and fluctuations, a realistic description of the dynamics is not possible. A solution could be to use quantum-mechanical considerations for estimating the mass tensor [86], the full friction tensor and the dependence of the entropy on the relevant degrees of freedom, including the excitation energy, and to perform the dynamical calculation with a stochastic approach. A step in this direction has already been made [204]. However, the Langevin equations are based on the assumption that all degrees of freedom of the environment form a heat bath, that means that they are in statistical equilibrium at every moment. This is probably not always a realistic assumption, and it might be necessary to take this into account.

The transformation of energy and the transport of heat between different subsystems during the fission process are genuine problems of statistical mechanics. It would be a great progress if considerations of statistical mechanics could be introduced into microscopic quantum-mechanical approaches in some manageable way.

The observation of gradual systematic variations of the fission quanti-

ties along neighboring nuclei may be exploited to increase the precision of microscopic models that treat each fissioning system independently with its own technical uncertainties that are inherent, for example in the shell effects determined with the Strutinsky procedure or in the potential energy determined in a restricted deformation space, discussed in section 5.1.2.

One may also extend the validity range of semi-empirical approaches like the GEF model, which covers a considerable variety of fission quantities, if one succeeds in deriving the justification for some approximations of the GEF model as well as for the values of the model parameters on a microscopic basis.

5.6 Experimental needs

In the field of nuclear fission, a process that is still so far from being fully understood, it is not possible to give a list of most important missing experimental information. One should be prepared for surprises and for new problems to emerge when new data come up. However, some general rules may be given. It is certainly beneficial to cover a range as wide as possible in the choice of the fissioning system in terms of nuclear composition (Z and A), excitation energy and angular momentum. Moreover, the coverage of fission observables should be as complete as possible, and they should be measured with a resolution as good as possible with as many quantities as possible in coincidence.

In the following, we will illustrate the relevance of the rules mentioned above by reminding the progress brought about by some specific experimental information or the open questions that could be answered by new measurements.

5.6.1 Wide coverage and precise definition of initial excitation energy

Distinguishing different fission chances: At energies that are above the threshold for multi-chance fission, the fission fragments are emitted from a wide range of excitation energy. Further development of suitable differential techniques [205] to distinguish the fission events from different fission chances will improve the experimental knowledge on the washing out of shell effects in the fission probability and the fission-fragment production with increasing excitation energy at fission.

Energy dependence of odd-even effect in different observables: The experimental information available at present about the decrease of the odd-even effect in fission-fragment Z distributions with increasing initial excitation energy has been obtained with relatively broad excitation-energy distributions, e.g. by bremsstrahlung-induced fission, e.g. ref. [206], or by electromagnetic-induced fission at relativistic energies [64]. First results on the energy dependence of the odd-even effect in fission-fragment N distributions has only been deduced very recently by comparing new data from electromagnetic-induced fission at relativistic energies [46] with results from thermal-neutron-induced fission, see section 3.3. The precise determination of the energy-dependent odd-even staggering in fission-fragment Z and N distributions, total kinetic energies and other observables would certainly help to better understand the influence of pairing correlations on the fission process.

5.6.2 Extended systematic coverage of fissioning systems

Shell structure in fragment distributions around $A = 200$: The observation of a double-humped mass distribution in the fission of ^{180}Hg [31] drew the attention to the appearance of structural effects in the fission of lighter fissioning nuclei ($A < 210$). In spite of intense experimental effort, a comprehensive overview on mass distributions in low-energy fission of these nuclei could not yet be established. The most efficient method to provide a wide systematics of fission-fragment mass distribution for fission from energies in the vicinity of the fission barrier of neutron-deficient systems over a large mass range is the electromagnetic-induced fission of relativistic projectile fragments that is presently used by the SOFIA experiment. New experimental results are urgently awaited.

Fragment distributions for long isotopic chains: The evolution of fragment mass distributions is of great interest for two reasons: Firstly, it will help to better estimate the mass distributions from the fission of very neutron-rich nuclei on the astrophysical r-process path. This information is urgently needed for simulating the nuclide production in the r-process. Secondly, the position of the mean Z in the heavy component of the asymmetric fission channels could be followed over a larger range. This could help to better understand the mechanism behind the surprisingly constant mean Z values in the heavy components of the fission-fragment distributions.

5.6.3 Correlations of as many observables as possible

The few data on the variation of the mass-dependent prompt-neutron multiplicities as a function of initial excitation energy are presently the only rather direct experimental evidence for the energy-sorting process. This illustrates the importance of multi-parameter experiments for discovering new features of the fission process. This concerns for example identification of fission fragments in A and Z and measurement of their kinetic energies, multiplicities and energies of prompt neutrons and prompt gammas. In general, such data will provide important constraints on the modeling of fission.

6 Summary

The experimental and the theoretical activities of the last years that have most strongly promoted the understanding of nuclear fission and the prospects for future developments have been covered in this review.

On the experimental side, the application of inverse kinematics extended the experimental capabilities in several aspects. At present, this is the only way that allows identifying all fission products in Z and A. In an approach developed at GSI, Darmstadt, fragmentation products from a relativistic ^{238}U beam were fully identified in Z and A and brought to fission by Coulomb excitation in a heavy target material. This technique allows to investigate low-energy fission of a large number of nuclei with $A \leq 238$ that were not accessible before. The fission products could be identified in Z and A with an excellent resolution. This technique has already proven its potential by mapping the transition from symmetric fission to asymmetric fission around ^{226}Th. But first results demonstrate that this technique also offers unique possibilities for systematic experiments on lighter neutron-deficient nuclei in an extended region around ^{180}Hg. In another approach, developed at GANIL, transfer reactions of a ^{238}U primary beam in a carbon target gave access to experiments on fission for a number of heavier nuclei with well defined excitation energy and separation of all fission products in Z and A. At CERN-ISOLDE, the progress in LASER ionization made it possible to study beta-delayed fission with fully identified ISOL beams and to discover the asymmetric fission of ^{180}Hg and structural effects in the mass distributions of other neighboring nuclei.

On the theoretical side, much effort is being invested in developing fully microscopic and quantum-mechanical, self-consistent, descriptions of the fission process. In spite of the difficulties caused by the high demand on computer power, the lack of suitable tools to handle non-equilibrium processes

and the difficulties of introducing phenomena of statistical mechanics into a quantum-mechanical description, progress is being made in promoting the qualitative understanding of fundamental aspects of nuclear fission. The dynamical TDSLDA approach that avoids any constraint on the collective variables and the study of quantum localization around scission are among the most interesting recent developments.

The stochastic description of the fission process by the numerical solution of the Langevin equations, after being successfully applied for many years for studying high-energy fission, has recently also been applied to low-energy fission, where shell effects and pairing correlations play an important role. The strength of this approach is the inherent treatment of statistical mechanics, the drawback is the classical character of the Langevin equation. Systematic dynamical calculations of the fission quantities and their variation as a function of the nuclear composition and the excitation energy are possible. Unfortunately, the necessity for Monte-Carlo sampling entails a limitation in the number of relevant degrees of freedom that are explicitly considered and, thus, a restriction in the coverage of fission quantities, or a strongly simplified treatment of the dynamics. A gradual extension is expected in line with the progress of computer technology.

Another possibility of modeling fission consists in the combination of powerful theoretical ideas and empirical knowledge. A rather successful example is the recently developed GEF model that is based on a global view on experimental findings and the application of general rules and ideas of physics and mathematics. It covers almost all fission observables and is able to reproduce measured data with high precision while having a remarkable predictive power by establishing and exploiting unexpected systematics and hidden regularities in the fission observables. This model revealed features that are not covered by current microscopic and self-consistent models, in particular several manifestations of statistical mechanics. A highlight is the discovery of energy sorting.

Acknowledgement

This work has been supported by the European Commission within the EURATOM FP7 Framework Programm through CHANDA (project no. 605203) and by the Nuclear Energy Agency of the OECD. One of the authors (K.-H. S.) acknowledges stimulating discussions with the participants of the program on Quantitative Large Amplitude Shape Dynamics: fission and heavy ion fusion that was held at the INT of the University of Washing-

ton in Seattle, Washington, from 23 September to 15 November, 2013. We thank Denis Lacroix for a critical reading of the section on self-consistent microscopic approaches, Aurel Bulgac for clarifications about the TDSLDA approach, and Christelle Schmitt for fruitful discussions. K.-H. S. thanks the CENBG for warm hospitality.

References

[1] M. Arnould, S. Goriely, K. Takahashi, "The r-process of stellar nucleosynthesis: Astrophysics and nuclear physics achievements and mysteries", Phys. Rep. 450 (2007) 97

[2] S. Goriely, "The fundamental role of fission during r-process nucleosynthesis in neutron star mergers", Eur. Phys. J. A 51 (2015) 22

[3] Joel de Jesús Mendoza-Temis, Meng-Ru Wu, Karlheinz Langanke, Gabriel Martínez-Pinedo, Andreas Bauswein, Hans-Thomas Janka, "Nuclear robustness of the r process in neutron-star mergers", Phys. Rev. C 92 (2015) 055805

[4] J.-P. Delaroche, M. Girod, H. Goutte, J. Libert, "Structure properties of even-even actinides at normal and super deformed shapes analysed using the Gogny force", Nucl. Phys. A 771 (2006) 103

[5] D. Jacquet, M. Morjean, "Fission times of excited nuclei: An experimental overview", Prog. Part. Nucl. Phys. 63 (2009) 155

[6] "Fission dynamics of intermediate-fissility systems: A study within a stochastic three-dimensional approach", E. Vardaci, P. N. Nadtochy, A. Di Nitto, A. Brondi, G. La Rana, R. Moro, P. K. Rath, M. Ashaduzzaman, E. M. Kozulin, G. N. Knyazheva, I. M. Itkis, M. Cinausero, G. Prete, D. Fabris, G. Montagnoli, N. Gelli, Phys. Rev. C 92 (2015) 034610

[7] K.-H. Schmidt, B. Jurado, "Entropy-driven excitation-energy sorting in superfluid fission dynamics", Phys. Rev. Lett. 104 (2010) 212501

[8] S. G. Kadmensky, "The quantum and thermodynamical characteristics of fission taking into account adiabatic and nonadiabatic modes of motion", Phys. Atom. Nuclei 70 (2007) 1628

[9] K. P. Santhosh, Sreejith Krishnan, B. Priyanka, "Isotopic yield in alpha accompanied ternary fission of ^{252}Cf", Int. J. Mod. Phys. E 24 (2015) 1550001

[10] J. P. Bondorf, "Chaotic fragmentation of nuclei", Nucl. Phys. A 387 (1982) 25c

[11] B. Borderie, M. F. Rivet, "Nuclear multifragmentation and phase transition for hot nuclei", Prog. Part. Nucl. Phys. 61 (2008) 551

[12] R. du Rietz, E. Williams, D. J. Hinde, M. Dasgupta, M. Evers, C. J. Lin, D. H. Luong, C. Simenel, A. Wakhle "Mapping quasifission characteristics and timescales in heavy element formation reactions" Phys. Rev. C 88 (2013) 054618

[13] F. H. Fröhner, "Evaluation and Analysis of Nuclear Resonance Data", JEFF Report **18**, NEA/DB/DOC(2000), NEA Data Bank of the OECD, 2000, available from `http://www.oecd-nea.org/dbdata/nds_jefreports/`.

[14] R. Capote, M. Herman, P. Obložinský, P. G. Young, S. Goriely, T. Belgya, A. V. Ignatyuk, A. J. Koning, S. Hilaire, V. A. Plujko, M. Avrigeanu, O. Bersillon, M. Chadwick, T. Fukahori, Zhigang Ge, Yinlu Han, S. Kailas, J. Kopecky, V. M. Maslov, G. Reffo, M. Sin, E. Sh. Soukhovitskii, P. Talou, "RIPL - Reference Input Parameter Library for Calculation of Nuclear Reactions and Nuclear Data Evaluations", Nucl. Data Sheets 110 (2009) 3107

[15] S. Goriely, S. Hilaire, A. J. Koning, R. Capote, "Towards an improved evaluation of neutron-induced fission cross sections on actinides", Phys. Rev. C 83 (2011) 034601

[16] P. Romain, B. Morillon, H. Duarte, "Bruyères-le-Châtel Neutron Evaluations of Actinides with the TALYS Code: the Fission Channel", Nucl. Data Sheets 131 (2016) 222

[17] F. Gönnenwein, "Neutron-induced fission", Lecture given at the Ecole Joliot Curie, 2014, Frejus, France, `http://ejc2014.sciencesconf.org/conference/ejc2014/pages/goennewein2.pdf`

[18] S. Kailas, K. Mahata, "Charged particle-induced nuclear fission reactions - progress and prospects", Pramana 83 (2014) 851

[19] S. S. Belyshev, B. S. Ishkhanov, A. A. Kuznetsov, K. A. Stopani, "Mass yield distributions and fission modes in photofission of ^{238}U below 20 MeV", Phys. Rev. C 91 (2015) 034603

[20] A. Gavron, H. C. Britt, E. Konecny, J. Weber, J. B. Wilhelmy, "Gamma(n)/Gamma(f) for actinide nuclei using (^{3}He,df) and (^{3}He,tf) reactions", Phys. Rev. C 13 (1976) 2374

[21] E. K. Hulet, J. F. Wild, R. J. Dougan, R. W. Lougheed, J. H. Landrum, A. D. Dougan, P. A. Baisden, C. M. Henderson, R. J. Dupzyk, "Spontaneous fission properties of ^{258}Fm, ^{260}Md, ^{258}No and ^{260}104: Bimodal fission", Phys. Rev. C 40 (1989) 770

[22] D. C. Hoffman, M. R. Lane, "Spontaneous fission", Radiochimica Acta 70/71 (1995) 135

[23] U. Brosa, S. Grossmann, A. Müller, "Nuclear scission", Phys. Rep. 197 (1990) 167

[24] H. Nifenecker, G. Mariolopoulos, J. P. Bocquet, R. Brissot, Mme Ch. Hamelin, J. Crancon, Ch. Ristori, "A combinatorial analysis of pair breaking in fission", Z. Phys. A 308 (1982) 39

[25] W. Nörenberg, "Unified theory of low-energy fission and fission models", Proc. Symp. Phys. Chem. Fission, Rochester 1973, IAEA Vienna (1974), vol. 1, p. 547

[26] B. D. Wilkins, E. P. Steinberg, R. R. Chasman, "Scission-point model of nuclear fission based on deformed-shell effects", Phys. Rev. C 14 (1976) 1832

[27] F. A. Ivanyuk, S. Chiba, Y. Aritomo, "Scission-point configuration within the two-center shell model shape parameterization", Phys. Rev. C 90 (2014) 054607

[28] J.-F. Lemaître, St. Panebianco, J.-L. Sida, St. Hilaire, S. Heinrich, "New statistical scission-point model to predict fission fragment observables", Phys. Rev. C 92 (2015) 034617

[29] N. Carjan, F. A. Ivanyuk, Yu. Oganessian, G. Ter-Akopian, "Fission of transactinide elements described in terms of generalized Cassinian ovals: Fragment mass and total kinetic energy distributions", Nucl. Phys. A 942 (2015) 97

[30] K. Nishio, A. Andreyev, K.-H. Schmidt, "Nuclear Fission: A Review of Experimental Advances and Phenomenology", to be published in Rep. Progr. Phys.

[31] A. N. Andreyev, M. Huyse, P. Van Duppen, "Colloquium: Beta-delayed fission of atomic nuclei", Rev. Mod. Phys. 85 (2013) 1541

[32] M. G. Itkis, V. N. Okolovich, A. Ya. Rusanov, G. N. Smirenkin, "Symmetric and asymmetric fission of nuclei lighter than thorium, Sov. J. Part. Nucl. 19 (1988) 301

[33] L. Ghys, A. N. Andreyev, M. Huyse, P. Van Duppen, S. Sels, B. Andel, S. Antalic, A. Barzakh, L. Capponi, T. E. Cocolios, X. Derkx, H. De Witte, J. Elseviers, D. V. Fedorov, V. N. Fedosseev, F. P. Hessberger, Z. Kalaninová, U. Köster, J. F. W. Lane, V. Liberati, K. M. Lynch, B. A. Marsh, S. Mitsuoka, P. Möller, Y. Nagame, K. Nishio, S. Ota, D. Pauwels, R. D. Page, L. Popescu, D. Radulov, M. M. Rajabali, J. Randrup, E. Rapisarda, S. Rothe, K. Sandhu, M. D. Seliverstov, A. M. Sjödin, V. L. Truesdale, C. Van Beveren, P. Van den Bergh, Y. Wakabayash, M. Warda, "Evolution of fission-fragment mass distributions in the neutron-deficient lead region", Phys. Rev. C 90 (2014) 041301(R)

[34] E. Prasad, D. J. Hinde, K. Ramachandran, E. Williams, M. Dasgupta, I. P. Carter, K. J. Cook, D. Y. Jeung, D. H. Luong, S. McNeil, C. S. Palshetkar, D. C. Rafferty, C. Simenel, A. Wakhle, J. Khuyagbaatar, Ch. E. Düllmann, B. Lommel, B. Kindler, "Observation of mass-asymmetric fission of mercury nuclei in heavy ion fusion", Phys. Rev. C 91 (2015) 064605

[35] R. Tripathi, S. Sodaye, K. Sudarshan, B. K. Nayak, A. Jhingan, P. K. Pujari, K. Mahata, S. Santra, A. Saxena, E. T. Mirgule, R. G. Thomas, "Fission fragment mass distributions in ^{35}Cl + ^{144,154}Sm reactions", Phys. Rev. C 92 (2015) 024610

[36] K. Nishio, A. N. Andreyev, R. Chapman, X. Derkx, Ch. E. Düllmann, L. Ghys, F. P. Hessberger, K. Hirose, H. Ikezoe, J. Khuyagbaatar, B. Kindler, B. Lommel, H. Makii, I. Nishinaka, T. Ohtsuki, S.D. Pain, R. Sagaidak, I. Tsekhanovich, M. Venhart, Y. Wakabayashi, S. Yan, "Excitation energy dependence of fragment-mass distributions from fission of ^{180,190}Hg formed in fusion reactions of ^{36}Ar + ^{144,154}Sm", Phys. Lett. B 748 (2015) 89

[37] A. V. Andreev, G. G. Adamian, N. V. Antonenko, A. N. Andreyev, "Isospin dependence of mass-distribution shape of fission fragments of Hg isotopes", Phys. Rev. C 88 (2013) 047604

[38] J. D. McDonnell, W. Nazarewicz, J. A. Sheikh, A. Staszczak, M. Warda, "Excitation-energy dependence of fission in the mercury region", Phys. Rev. C 90 (2014) 021302(R)

[39] Stefano Panebianco, Jean-Luc Sida, Héloise Goutte, Jean-Franois Lemaître, Noël Dubray, Stéphane Hilaire, "Role of deformed shell effects on the mass asymmetry in nuclear fission of mercury isotopes", Phys. Rev. C 86 (2012) 064601

[40] M. Warda, A. Staszczak, W. Nazarewicz, "Fission modes of mercury isotopes", Phys. Rev. C 86 (2012) 024601

[41] Jutta E. Escher, Jason T. Burke, Frank S. Dietrich, Nicholas D. Scielzo, Ian J. Thompson, Walid Younes, "Compound-nuclear reaction cross sections from surrogate measurements", Rev. Mod. Phys. 84 (2012) 353

[42] K. Nishio, Contribution to the workshop INT 13-3, Seattle, 14-18 Oct. 2013,

[43] C. Rodríguez-Tajes, F. Farget, X. Derkx, M. Caamaño, O. Delaune, K. -H. Schmidt, E. Clément, A. Dijon, A. Heinz, T. Roger, L. Audouin, J. Benlliure, E. Casarejos, D. Cortina, D. Doré, B. Fernández-Domínguez, B. Jacquot, B. Jurado, A. Navin, C. Paradela, D. Ramos, P. Romain, M. D. Salsac, C. Schmitt, "Transfer reactions in inverse kinematics, an experimental approach for fission investigations", Phys. Rev. C 89 (2014) 024614

[44] F. Farget, M. Caamaño, D. Ramos, C. Rodríguez-Tajes, K.-H. Schmidt, L. Audouin, J. Benlliure, E. Casarejos, E. Clément, D. Cortina, O. Delaune, X. Derkx, A. Dijon, D. Doré, B. Fernández-Domínguez, L. Gaudefroy, C. Golabek, A. Heinz, B. Jurado, A. Lemasson, C. Paradela, T. Roger, M. D. Salsac, C. Schmitt, "Transfer-induced fission in inverse kinematics: Impact on experimental and evaluated nuclear data bases", Eur. Phys. J. A 51 (2015) 175

[45] K.-H. Schmidt, S. Steinhäuser, C. Böckstiegel, A. Grewe, A. Heinz, A. R. Junghans, J. Benlliure, H.-G. Clerc, M. de Jong, J. Müller, M.

Pfützner, B. Voss, "Relativistic radioactive beams: A new access to nuclear-fission studies", Nucl. Phys. A 665 (2000) 221

[46] G. Boutoux, G. Bélier, A. Chatillon, A. Ebran, T. Gorbinet, B. Laurent, J.-F. Martin, E. Pellereau, J. Taïeb, L. Audouin, L. Tassan-Got, B. Jurado, H. Alvarez-Pol, Y. Ayyad, J. Benlliure, M. Caamaño, D. Cortina-Gil, B. Fernández-Domínguez, C. Paradela, J.-L. Rodríguez-Sànchez, J. Vargas, E. Casarejos, A. Heinz, A. Kelić-Heil, N. Kurz, C. Nociforo, S. Pietri, A. Prochazka, D. Rossi, K.-H. Schmidt, H. Simon, B. Voss, H. Weick, J. S. Winfield, "The SOFIA experiment", Physics Procedia 47 (2013) 166

[47] Julie-Fiona Martin, Julien Taïeb, Audrey Chatillon, Gilbert Bélier, Guillaume Boutoux, Adeline Ebran, Thomas Gorbinet, Lucie Grente, Benoit Laurent, Eric Pellereau, Héctor Alvarez-Pol, Laurent Audouin, Thomas Aumann, Yassid Ayyad, Jose Benlliure, Enrique Casarejos, Dolores Cortina Gil, Manuel Caamaño, Fanny Farget, Beatriz Fernández Domínguez, Andreas Heinz, Beatriz Jurado, Aleksandra Kelić-Heil, Nikolaus Kurz, Chiara Nociforo, Carlos Paradela, Stéphane Pietri, Diego Ramos, Jose-Luis Rodríguez-Sànchez, Carme Rodríguez-Tajes, Dominic Rossi, Karl-Heinz Schmidt, Haik Simon, Laurent Tassan-Got, Jossitt Vargas, Bernd Voss, Helmut Weick, "Studies on fission with ALADIN - Precise and simultaneous measurement of fission yields, total kinetic energy and total prompt neutron multiplicity at GSI", Eur. Phys. J. A 51 (2015) 174

[48] E. A. C. Crough, "Fission-product yields from neutron-induced fission", At. Data Nucl. Data Tables 19 (1977) 417

[49] J. Laurec, A. Adam, T. de Bruyne, E. Bauge, T. Granier, J. Aupiais, O. Bersillon, G. Le Petit, N. Authier, P. Casoli, "Fission product yields of ^{233}U, ^{235}U, ^{238}U and ^{239}Pu in fields of thermal neutrons, fission neutrons and 14.7-MeV neutrons", Nucl. Data Sheets 111 (2010) 2965

[50] W. E. Stein, "Velocities of fragment pairs from ^{233}U, ^{235}U, and ^{239}Pu fission", Phys. Rev. 108 (1957) 94

[51] J. C. D. Milton, J. S. Fraser, "Spontaneous fission fragment velocity measurements and coincident gamma spectra for Cf252", Phys. Rev. 111 (1958) 877

[52] H. W. Schmitt, W. E. Kiker, C. W. Williams, "Precision measurements of correlated energies and velocities of ^{252}Cf fission fragments", Phys. Rev. 137 (1965) B837

[53] A. Öd, P. Geltenbort, R. Brissot, F. Gönnenwein, P. Perrin, E. Aker, D. Engelhardt, "A mass spectrometer for fission fragments based on time-of-flight and energy measurements", Nucl. Instrum. Methods 219 (1984) 569

[54] A. Sicre, G. Barreau, A. Boukellai, F. Caitucoli, T. P. Oan, B. Leroux, P. Geltenbort, F. Gönnenwein, A. Öd, M. Asghar, "High-resolution study of ^{235}U(nth,f) and ^{229}Th(nth,f) with cosi fan tutte mass spectrometer", Rad. Eff. 93 (1986) 65

[55] E. Moll, H. Schrader, G. Siegert, M. Asghar, J. P. Bocquet, G. Bailleul, J. P. Gautheron, J. Greif, G. I. Crawford, C. Chauvin, H. Ewald, H. Wollnik, P. Armbruster, G. Fiebig, H. Lawin, K. Sistemich, "Analysis of ^{236}U-fission products by the recoil separator 'Lohengrin'", Nucl. Instrum. Methods 123 (1975) 615

[56] Taofeng Wang, Hongyin Han, Qinghua Meng, Liming Wang, Liping Zhu, Haihong Xia, "Measurements of charge distributions of the fragments in the low energy fission reaction", Nucl. Instrum. Methods A 697 (2013) 7

[57] K. Meierbachtol, F. Tovesson, D. Shields, C. Arnold, R. Blakeley, T. Bredeweg, M. Devlin, A. A. Hecht, L. E. Heffern, J. Jorgenson, A. Laptev, D. Mader, J. M. O'Donnell, A. Sierk, M. White, "The SPIDER fission fragment spectrometer for fission product yield measurements", Nucl. Instrum. Methods A 788 (2015) 59

[58] M. O. Frégeau, S. Oberstedt, "The Fission-fragment Spectrometer VERDI", Physics Procedia 64 (2015) 197

[59] I. Tsekhanovich, J. A. Dare, A. G. Smith, B. Varley, D. Cullen, N. Lumley, T. Materna, U. Köster, G.S. Simpson, "A Novel 2v2E Spectrometer in Manchester. New development in Identification of fission fragments", Proceedings of the "Seminar on fission", Corsendonk Priory, Belgium, 18-21 September 2007, World Scientific, Editors Cyriel Wagemans, Jan Wagemans and Pierre D'hondt

[60] Stefano Panebianco, Diane Doré, Fanny Farget, Francois-Rene Lecolley, Gregory Lehaut, Thomas Materna, Julien Pancin, Thomas Papaevangelou, "FALSTAFF: a novel apparatus for fission fragment characterization", EPJ Web of Conferences 69 (2014) 00021

[61] M. Caamaño, O. Delaune, F. Farget, X. Derkx, K.-H. Schmidt, L. Audouin, C.-O. Bacri, G. Barreau, J. Benlliure, E. Casarejos, A. Chbihi, B. Fernández-Domínguez, L. Gaudefroy, C. Golabek, B. Jurado, A. Lemasson, A. Navin, M. Rejmund, T. Roger, A. Shrivastava, C. Schmitt, "Isotopic yield distributions of transfer- and fusion-induced fission from ^{238}U+^{12}C reactions in inverse kinematics", Phys. Rev. C 88 (2013) 024605

[62] A. Navin, M. Rejmund, C. Schmitt, S. Bhattacharyya, G. Lhersonneau, P. Van Isacker, M. Caamaño, E. Clément, O. Delaune, F. Farget, G. De France, B. Jacquot, "Towards the high spin-isospin frontier using isotopically-identified fission fragments", Phys. Lett. B 728 (2014) 136

[63] C. Böckstiegel, S. Steinhäuser, K.-H. Schmidt, H.-G. Clerc, A. Grewe, A. Heinz, M. de Jong, A. R. Junghans, J. Müller, B. Voss, "Nuclear-fission studies with relativistic secondary beams: analysis of fission channels", Nucl. Phys. A 802 (2008) 12

[64] S. Steinhäuser, J. Benlliure, C. Böckstiegel, H.-G. Clerc, A. Heinz, A. Grewe, M. de Jong, A. R. Junghans, J. Müller, M. Pfützner, K.-H. Schmidt, "Odd-even effects observed in the fission of nuclei with unpaired protons", Nucl. Phys. A 634 (1998) 89

[65] M. Caamaño, F. Rejmund, K.-H. Schmidt, "Evidence for the predominant influence of the asymmetry degree of freedom on the even-odd structure in fission-fragment yields", J. Phys. G: Nucl. Part. Phys. 38 (2011) 035101

[66] B. L. Tracy, J. Chaumont, R. Klapisch, J. M. Nitschke, A. M. Poskanzer, E. Roeckl, C. Thibault, "Rb and Cs isotopic cross sections from 40-60-MeV-proton fission of ^{238}U, ^{232}Th, and ^{235}U", Phys. Rev. C 5 (1972) 222

[67] E. Pellereau, PhD thesis, université de Paris Sud, 2013 (in French)

[68] W. Lang, H.-G. Clerc, H. Wohlfarth, H. Schrader, K.-H. Schmidt, "Nuclear charge and mass yields for ^{235}U(n_{th},f) as a function of the kinetic energy of the fission products", Nucl. Phys. A 345 (1980) 34

[69] F. Gönnenwein, "On the notion of odd-even effects in the yields of fission fragments", Nucl. Instr. Meth. A 316 (1992) 405

[70] M. Caamaño, O. Delaune, F. Farget, X. Derkx, K.-H. Schmidt, L. Audouin, C.-O. Bacri, G. Barreau, J. Benlliure, E. Casarejos, A. Chbihi, B. Fernández-Domínguez, L. Gaudefroy, C. Golabek, B. Jurado, A. Lemasson, A. Navin, M. Rejmund, T. Roger, A. Shrivastava, C. Schmitt, "Isotopic yield distributions of transfer- and fusion-induced fission from ^{238}U+^{12}C reactions in inverse kinematics", Phys. Rev. C 88 (2013) 024605

[71] D. Ramos, C. Rodrguez-Tajes, M. Caamano, F. Farget, L. Audouin, J. Benlliure, E. Casarejos, E. Clement, D. Cortina, O. Delaune, X. Derkx, A. Dijon, D. Dore, B. Fernandez-Dominguez, G. de France, A. Heinz, B. Jacquot, A. Navin, C. Paradela, M. Rejmund, T. Roger, M. D. Salsac, C. Schmitt, "Dependence of fission-fragment properties on excitation energy for neutron-rich actinides", EPJ Web of Conferences 111 (2016) 10001

[72] M. Caamaño, F. Farget, O. Delaune, K.-H. Schmidt, C. Schmitt, L. Audouin, C.-O. Bacri, J. Benlliure, E. Casarejos, X. Derkx, B. Fernández-Domínguez, L. Gaudefroy, C. Golabek, B. Jurado, A. Lemasson, D. Ramos, C. Rodriguez-Tajes, T. Roger, A. Shrivastava, "Characterization of the scission point from fission-fragment velocities", Phys. Rev. C 92 (2015) 034606

[73] A. Chatillon for the SOFIA collaboration, "SOFIA: Studies on fission with Aladin", Contr. to the 22nd ASRC International Workshop "Nuclear Fission and Exotic Nuclei", December 3-5, 2014, Japan Atomic Energy Agency (JAEA), Tokai, Japan

[74] H. J. Krappe, K. Pomorski, "Theory of Nuclear Fission", Lecture Notes in Physics 838, Springer, Heidelberg, 2012

[75] R. Machleidt, D. R. Entem, "Chiral effective field theory and nuclear force", Phys. Rep. 503 (2011) 1

[76] J. W. Negele, "Microscopic theory of fission dynamics", Nucl. Phys. A 502 (1989) 371c

[77] Denis Lacroix, "Quantum nuclear many-body dynamics and related aspects", habilitation thesis, 2010, http://pro.ganil-spiral2.eu/laboratory/research/theory/members/denis/hdr/

[78] Philip Goddard, Paul Stevenson, Arnau Rios, "Fission dynamics within time-dependent Hartree-Fock: Deformation-induced fission", Phys. Rev. C 92 (2015) 054610

[79] A. Bulgac, P. Magierski, K. J. Roche, I. Stetcu, "Induced fission of ^{240}Pu within a real-time microscopic framework", Phys. Rev. Lett. 116 (2016) 122504

[80] A. Staszczak, A. Baran, J. Dobaczewski, W. Nazarewicz, "Microscopic description of complex nuclear decay: Multimodal fission", Phys. Rev. C 80 (2009) 014309

[81] Jhilam Sadhukhan, J. Dobaczewski, W. Nazarewicz, J. A. Sheikh, A. Baran, "Pairing-induced speedup of nuclear spontaneous fission", Phys. Rev. C 90 (2014) 061304(R)

[82] H. Goutte, J. F. Berger, P. Casoli, D. Gogny, "Microscopic approach of fission dynamics applied to fragment kinetic energy and mass distributions in ^{238}U", Phys. Rev. C 71 (2005) 024316

[83] A. C. Wahl, Los Alamos National Laboratory Report N. LA-13928, 2002 (unpublished)

[84] C. Simenel, A. S. Umar, "Formation and dynamics of fission fragments", Phys. Rev. C 89 (2014) 031601(R)

[85] Guillaume Scamps, Cédric Simenel, Denis Lacroix, "Superfluid dynamics of ^{258}Fm fission", Phys. Rev. C 92 (2015) 011602(R)

[86] Yusuke Tanimura, Denis Lacroix, Guillaume Scamps, "Collective aspects deduced from time-dependent microscopic mean-field with pairing: Application to the fission process", Phys. Rev. C 92 (2015) 034601

[87] R. Bernard, H. Goutte, D. Gogny, W. Younes, "Microscopic and nonadiabatic Schrödinger equation derived from the generator coordinate method based on zero- and two-quasiparticle states", Phys. Rev. C 84 (2011) 044308

[88] W. Younes, D. Gogny, "Nuclear scission and quantum localization", Phys. Rev. Lett. 107 (2011) 132501

[89] N. Schunck, D. Duke, H. Carr, A. Knoll, "Description of induced nuclear fission with Skyrme energy functionals: Static potential energy surfaces and fission fragment properties", Phys. Rev. C 90 (2014) 054305

[90] N. Schunck, D. Duke, H. Carr, "Description of induced nuclear fission with Skyrme energy functionals. II. Finite temperature effects", Phys. Rev. C 91 (2015) 034327

[91] Philip Goddard, Paul Stevenson, Arnau Rios, "Fission dynamics within time-dependent Hartree-Fock. II. Boost-induced fission", Phys. Rev. C 93 (2016) 014620

[92] R. Rodríguez-Guzmán, L. M. Robledo, "Microscopic description of fission in uranium isotopes with the Gogny energy density functional", Phys. Rev. C 89 (2014) 054310

[93] R. Rodríguez-Guzmán, L. M. Robledo, "Microscopic description of fission in neutron-rich radium isotopes with the Gogny energy density functional", Eur. Phys. J. A 52 (2016) 12

[94] J. R. Nix, "Further studies in the liquid-drop theory on nuclear fission", Nucl. Phys. A 130 (1969) 241

[95] K. T. R. Davies, A. J. Sierk, J. R. Nix, "Effect of viscosity on the dynamics of fission", Phys. Rev. C 13 (1976) 2385

[96] G. D. Adeev, I. I. Gonchar, V. V. Pashkevich, N. I. Pischasov, O. I. Serdyuk, "Diffusion model of the formation of fission-fragment distributions", Sov. J. Part. Nucl. 19 (1988) 529

[97] Y. Abe, C. Grégoire, H. Delagrange, "Langevin approach to nuclear dissipation dynamics", J. Phys. C 4 (47) (1986) 329

[98] A. Einstein, "Über die von der molekularkinetischen Theorie der Wärme geforderte Bewegung von in ruhenden Flüssigkeiten suspendierten Teilchen", Ann. Phys. (Leipzig) 322 (1905) 549

[99] P. Fröbrich, I. I. Gontchar, "Langevin description of fusion, deep-inelastic collisions and heavy-ion-induced fission", Phys. Rep. 292 (1998) 131

[100] P. Fröbrich, "On the dynamics of fission of hot nuclei", Nucl. Phys. A 787 (2007) 170c

[101] N. Metropolis, A. Rosenbluth, M. Rosenbluth, A. Teller, E. Teller, "Equations of state calculations by fast computing machines", J. Chem. Phys. 21 (1953) 1087

[102] T. Ichikawa, T. Asano, T. Wada, M. Ohta, "Dynamics of Fission Modes Studied with the 3-dimensional Langevin Equation", J. Nucl. Radioch. Sci. 3 (2002) 67

[103] D. Scharnweber, W. Greiner, U. Mosel, "The two-center shell model", Nucl. Phys. A 164 (1971) 257

[104] H.-J. Krappe, J. R. Nix, A. J. Sierk, "Unified nuclear potential for heavy-ion elastic scattering, fusion, fission, and ground-state masses and deformations", Phys. Rev. C 20 (1979) 992

[105] J. R. Nix, A. J. Sierk, "Calculation of compound-nucleus cross sections for symmetric very-heavy-ion reactions", Phys. Rev. C 15 (1977) 2072

[106] T. Asano, T. Wada, M. Ohta, T. Ichikawa, S. Yamaji, H. Nakahara, "Dynamical calculation of multi-modal nuclear fission of fermium nuclei", J. Nucl. Radioch. Sc. 5 (2004) 1

[107] T. Asano, T. Wada, M. Ohta, S. Yamaji, H. Nakahara, "The dependency on the dissipation tensor of multi-modal nuclear fission", J. Nucl. Radioch. Sc. 7 (2006) 7

[108] Y. Aritomo, S. Chiba, "Fission process of nuclei at low excitation energies with a Langevin approach", Phys. Rev. C 88 (2013) 044614

[109] K. Katakura, JENDL FP Decay Data File 2011 and Fission Yields Data File 2011, (Japan Atomic Energy Agency, 2012)

[110] Y. Aritomo, S. Chiba, F. Ivanyuk, "Fission dynamics at low excitation energy", Phys. Rev. C 90 (2014) 054609

[111] P. Möller, D. G. Madland, A. J. Sierk, A. Iwamoto, "Nuclear fission modes and fragment mass asymmetries in a five-dimensional deformation space", Nature 409 (2001) 785

[112] J. Randrup, P. Möller, "Brownian Shape Motion on Five-Dimensional Potential-Energy Surfaces: Nuclear Fission-Fragment Mass Distributions", Phys. Rev. Lett. 106 (2011) 13250

[113] J. Randrup, P. Möller, A. J. Sierk, "Fission-fragment mass distributions from strongly damped shape evolution", Phys. Rev. C 84 (2011) 034613

[114] P. Möller, J. Randrup, A. J. Sierk, "Calculated fission yields of neutron-deficient mercury isotopes", Phys. Rev. C 85 (2012) 024306

[115] J. Randrup, P. Möller, "Energy dependence of fission-fragment mass distributions from strongly damped shape evolution", Phys. Rev. C 88 (2013) 064606

[116] Peter Möller, Takatoshi Ichikawa, "A method to calculate fission-fragment yields $Y(Z, N)$ versus proton and neutron number in the Brownian shape-motion model", Eur. Phys. J. A 51 (2015) 173

[117] P. Möller, J. Randrup, "Calculated fission-fragment yield systematics in the region $74 \leq Z \leq 94$ and $90 \leq N \leq 150$", Phys. Rev. C 91 (2015) 044316

[118] M. Mirea, "Microscopic description of the odd-even effect in cold fission", Phys. Rev. C 89 (2014) 034623

[119] M. Mirea, R. C. Bobulescu, "Cranking mass parameters for fission", J. Phys. G: Nucl. Part. Phys. 37 (2010) 055106

[120] K.-H. Schmidt, B. Jurado, Ch. Amouroux, "General description of fission observables, GEF model", JEFF Report **24**, NEA/DB/DOC(2014)1, NEA Data Bank of the OECD, 2014, available from `http://www.oecd-nea.org/dbdata/nds_jefreports/`.

[121] K.-H. Schmidt, B. Jurado, Ch. Amouroux, "General description of fission observables, GEF model", Supplement to JEFF Report **24**, NEA/DB/DOC(2014)2, NEA Data Bank of the OECD, 2014, available from `http://www.oecd-nea.org/databank/docs/2014/`.

[122] K.-H. Schmidt, B. Jurado, C. Amouroux, C. Schmitt, "General description of fission observables: GEF model code", Nucl. Data Sheets 131 (2016) 107

[123] W. D. Myers, W. J. Swiatecki, "Nuclear properties according to the Thomas-Fermi model", Nucl. Phys. A 601 (1996) 141

[124] K.-H. Schmidt, B. Jurado, "Revealing hidden regularities with a general approach to fission", Eur. Phys. J. A 51 (2015) 176

[125] A. V. Karpov, A. Kelic, K.-H. Schmidt, "On the topographical properties of fission barriers", J. Phys. G: Nucl. Part. Phys. 35 (2008) 035104

[126] W. J. Świątecki, K. Siwek-Wilczyńska, J. Wilczyński, "Effect of shell structure on saddle point masses", Acta Phys. Pol. B 38 (2007) 1565

[127] M. Dahlinger, D. Vermeulen, K.-H. Schmidt, "Empirical saddle-point and ground-state masses as a probe of the droplet model", Nucl. Phys. A 376 (1982) 94

[128] A. Kelić, K.-H. Schmidt, "Assessment of saddle-point-mass predictions for astrophysical applications", Phys. Lett. B 634 (2006) 362

[129] W. D. Myers, W. J. Swiatecki, "Thomas-Fermi fission barriers", Phys. Rev. C 60 (1999) 014606

[130] S. Bjørnholm, J. E. Lynn, "The double-humped fission barrier", Rev. Mod. Phys. 52 (1980) 725

[131] P. Möller, A. J. Sierk, T. Ichikawa, A. Iwamoto, R. Bengtsson, H. Uhrenholt, S. Åberg, "Heavy-element fission barriers", Phys. Rev. C 79 (2009) 064304

[132] M. Kowal, P. Jachimowicz, A. Sobiczewski, "Fission barriers for even-even superheavy nuclei", Phys. Rev. C 82 (2010) 014303

[133] Takatoshi Ichikawa, Akira Iwamoto, Peter Möller, "Origin of the narrow, single peak in the fission-fragment mass distribution for 258Fm", Phys. Rev. C 79 (2009) 014305

[134] U. Mosel, H. W. Schmitt, "Potential energy surfaces for heavy nuclei in the two-center model", Nucl. Phys. A 165 (1971) 73

[135] K.-H. Schmidt, A. Kelić, M. V. Ricciardi, "Experimental evidence for the separability of compound-nucleus and fragment properties in fission", Europh. Lett. 83 (2008) 32001

[136] M. G. Itkis, V. N. Okolovich, A. Ya, Rusanov, G. N. Smirenkin, "Asymmetric fission of the pre-actinide nuclei", Z. Phys. A 320 (1985) 433

[137] E. Wigner, "The transition state method", Trans. Faraday Sot. 34 (1938) 29

[138] D. H. E. Gross, "Challenges about entropy", Contr. XILV Intern. Winter Meeting on Nuclear Physics, Bormio, Italy (2006), http://arxiv.org/abs/nucl-th/0603028

[139] M. Diebel, K. Albrecht, R. W. Hasse, "Microscopic calculations of fission barriers and critical angular momenta for excited heavy nuclear systems", Nucl. Phys. A 355 (1981) 66

[140] J. C. Pei, W. Nazarewicz, J. A. Sheikh, A. K. Kerman, "Fission barriers of compound superheavy nuclei", Phys. Rev. Lett. 102 (2009) 192501

[141] V. V. Pashkevich, A. Ya. Rusanov, "The ^{226}Th fission valleys", Nucl. Phys. A 810 (2008) 77

[142] Yu. Ts. Oganessian, Yu. A. Lazarev, Heavy ions and nuclear fission, in Treatise on Heavy Ion Science, Vol. 4, ed. D. A. Bromley, Plenum Press, New York, 1985, p. 1.

[143] G. D. Adeev, V. V. Pashkevich, "Theory of macroscopic fission dynamics", Nucl. Phys. A 502 (1989) 405c

[144] A. V. Karpov, P. N. Nadtochy, D. V. Vanin, G. D. Adeev, "Three-dimensional Langevin calculations of fission fragment mass-energy distribution from excited compound nuclei", Phys. Rev. C 63 (2001) 054610

[145] H. Nifenecker, "A dynamical treatment of isobaric widths in fission: An example of frozen quantal fluctuations", J. Physique Lett. 41 (1980) 47

[146] M. Asghar, "Charge distribution in fission - a quantum mechanical phenomenon", Z. Phys. A 296 (1980) 79

[147] W. D. Myers, G. Manzouranis, J. Randrup, "Adiabaticity criterion for charge equilibration with application to fission", Phys. Lett. B 98 (1981) 1

[148] A. V. Karpov, G. D. Adeev, "Langevin description of charge fluctuations in fission of highly excited nuclei", Eur. Phys. J. A 14 (2002) 169

[149] A. Ya. Rusanov, V. V. Pashkevich, M. G. Itkis, "Asymmetric fission barriers for hot rotating nuclei and experimental mass distributions of fission fragments, Phys. At. Nucl. 62 (1999) 547

[150] J. P. Unik, J. E. Gindler, L. E. Glendenin, K. F. Flynn, A. Gorski, R. K. Sjoblom, "Fragment mass and kinetic energy distributions for fissioning systems ranging from mass 230 to 256", Proc. Symp. Phys. Chem. Fission, Rochester 1973, IAEA Vienna (1974), vol. 2, p. 19

[151] D. M. Gorodisskiy, S. I. Mulgin, A. Ya. Rusanov, S. V. Zhdanov, "Isotopic invariance of fission-fragment charge distributions for actinite nuclei at excitation energies above 10 MeV", Phys. Atom. Nuclei 66 (2003) 1190

[152] T. R. England, B. F. Rider, Evaluation and compilation of fission product yields, ENDF-349, LA-UR-94-3106, Los Alamos National Laboratory (1994); Available from `http://t2.lanl.gov/publications/yields/apxA.txt`

[153] M. Asghar, R. W. Hasse, "Saddle-to-scission landscape in fission: Experiments and theories", J. Phys. Colloques 45 (1984) C6-455 - C6-462

[154] A. Gilbert, A. G. W. Cameron, "A composite nuclear-level density formula with shell corrections", Can. J. Phys. 43 (1965) 1446

[155] A. V. Ignatyuk, G. N. Smirenkin, A. S. Tiskin, "Phenomenological description of the energy dependence of the level density parameter", Sov. J. Nucl. Phys. 21 (1975) 255

[156] M. I. Svirin, "Testing basic phenomenological models of nuclear level density", Phys. Part. Nuclei 37 (2006) 475

[157] T. von Egidy, D. Bucurescu, "Experimental energy-dependent nuclear spin distributions", Phys. Rev. C 80 (2009) 054310

[158] K. Van Houcke, S. M. A. Rombouts, K. Heyde, Y. Alhassid, "Microscopic calculation of symmetry projected nuclear level densities", Phys. Rev. C 79 (2009) 024302

[159] S. Hilaire, M. Girod, S. Goriely, A. J. Koning, "Temperature-dependent combinatorial level densities with the D1M Gogny force", Phys. Rev. C 86 (2012) 064317 (10 pages)

[160] M. Bonett-Matiz, Abhishek Mukherjee, Y. Alhassid, "Level densities of nickel isotopes: Microscopic theory versus experiment", Phys. Rev. C 88 (2013) 011302(R)

[161] M. I. Svirin, "Testing basic phenomenological models of nuclear level density", Phys. Part. Nuclei 37 (2006) 475

[162] "Global and local level density models", A. J. Koning, S. Hilaire, S. Goriely, Nucl. Phys. A 810 (2008) 13-

[163] K.-H. Schmidt, B. Jurado, "Inconsistencies in the description of pairing effects in nuclear level densities", Phys. Rev. C 86 (2012) 044322

[164] L. G. Moretto, "Statistical description of a paired nucleus with the inclusion of angular momentum", Nucl. Phys. A 185 (1972) 145

[165] M. Guttormsen , M. Aiche, F. L. Bello Garrote, L. A. Bernstein, D. L. Bleuel, Y. Byun, Q. Ducasse, T. K. Eriksen, F. Giacoppo, A. Görgen, F. Gunsing, T. W. Hagen, B. Jurado, M. Klintefjord, A. C. Larsen, L. Lebois, B. Leniau, H. T. Nyhus, T. Renstrom, S. J. Rose, E. Sahin, S. Siem, T. G. Tornyi, G. M. Tveten, A. Voinov, M. Wiedeking, J. Wilson, "Experimental level densities of atomic nuclei", Eur. Phys. J. A 51 (2015) 170

[166] L. G. Moretto, A. C. Larsen, F. Giacoppo, M. Guttormsen, S. Siem, "Experimental first order pairing phase transition in atomic nuclei", J. Phys. Conf. Series 580 (2015) 012048

[167] A. V. Ignatyuk, "Systematics of Low-Lying Level Densities and Radiative Widths", Hadrons Nuclei Appl. 3 (2001) 287

[168] V. M. Strutinskii, Int. Conf. on Nuclear Physics (Paris, 1958) p. 617

[169] H. A. Bethe, "An attempt to calculate the number of energy levels of a heavy nucleus", Phys. Rev. 50 (1936) 332

[170] M. G. Itkis, K. G. Kuvatov, V. N. Okolovich, et al., Sov. J. Nucl. Phys. 16 (1973) 144

[171] K.-H. Schmidt, B. Jurado, "Thermodynamics of nuclei in thermal contact", Phys. Rev. C 83 (2011) 014607

[172] K.-H. Schmidt, B. Jurado, "Final excitation energy of fission fragments", Phys. Rev. C 83 (2011) 061601(R)

[173] H. C. Britt, S. L. Whetstone Jr., "Alpha-particle-induced fission of ^{230}Th, ^{232}Th and ^{233}U", Phys. Rev. 133 (1964) B603

[174] E. Cheifetz, Z. Fraenkel, "Prompt neutrons from fission of ^{238}U induced by 12 MeV protons", Phys. Rev. Lett. 21 (1968) 36

[175] E. Cheifetz, Z. Fraenkel, J. Galin, M. Lefort, J. Peter, X. Tarrago, "Measurement of the prompt neutrons emitted in the fission of ^{209}Bi and ^{238}U induced by 155-MeV protons", Phys. Rev. C 2 (1970) 256

[176] S. C. Burnett, R. L. Ferguson, F. Plasil, H. W. Schmitt, "Neutron emission and fission energetics in the proton-induced fission of ^{233}U and ^{238}U", Phys. Rev. C 3 (1970) 2034

[177] C. J. Bishop, R. Vandenbosch, R. Aley, R. W. Shaw Jr., I. Halpern, "Excitation energy dependence of neutron yields and fragment kinetic energy release in the proton-induced fission of ^{233}U and ^{238}U", Nucl. Phys. A 150 (1970) 129

[178] A. C. Wahl, "Systematics of fission product yields", in "Fission product yield data for the transmutation of minor actinide nuclear waste", IAEA, Vienna, Austria, STI/PUB/1286, 2008, pp. 117

[179] R. Müller, A. A. Naqvi, F. Käppeler, F. Dickmann, "Fragment velocities, energies and masses from fast neutron induced fission of ^{235}U", Phys. Rev. C 29 (1984) 885

[180] A. A. Naqvi, F. Käppeler, F. Dickmann, R. Müller, "Fission fragment properties in fast-neutron-induced fission of ^{237}Np", Phys. Rev. C 34 (1986) 218

[181] H. J. Krappe, S. Fadeev, "Pairing correlations around scission", Nucl. Phys. A 690 (2001) 431

[182] B. Jurado, K.-H. Schmidt, "Influence of complete energy sorting on the characteristics of the odd-even effect in fission-fragment element distributions", J. Phys. G: Nucl. Part. Phys. 42 (2015) 055101

[183] Peter Möller, Jørgen Randrup, Akira Iwamoto, Takatoshi Ichikawa, "Fission-fragment charge yields: Variation of odd-even staggering with element number, energy, and charge asymmetry", Phys. Rev. C 90 (2014) 014601

[184] M. V. Ricciardi, A. V. Ignatyuk, A. Kelić, P. Napolitani, F. Rejmund, K.-H. Schmidt, O. Yordanov, "Complex nuclear-structure phenomena revealed from the nuclide production in fragmentation reactions", Nucl. Phys. A 733 (2004) 299

[185] M. V. Ricciardi, K.-H. Schmidt, A. Kelić-Heil, "Even-odd effect in multifragmentation products: the footprints of evaporation", arXiv:1007.0386v2 [nucl-ex] (2011)

[186] B. Mei, H. S. Xu, X. L. Tu, Y. H. Zhang,Yu. A. Litvinov, K.-H. Schmidt, M. Wang, Z. Y. Sun, X. H. Zhou, Y. J. Yuan, M. V. Ricciardi, A. Kelić-Heil, R. Reifarth, K. Blaum, R. S. Mao, Z. G. Hu, P. Shuai, Y. D. Zang, Y. W. Ma, X. Y. Zhang, J. W. Xia, G. Q. Xiao, Z. Y. Guo, J. C. Yang, X. H. Zhang, X. Xu, X. L. Yan, W. Zhang, W. L. Zhan, "Origin of odd-even staggering in fragment yields: Impact of nuclear pairing and shell structure on the particle-emission threshold energy", Phys. Rev. C 89 (2014) 054612

[187] C. Schmitt, K.-H. Schmidt, A. Kelić-Heil, "SPACS: A semi-empirical parameterization for isotopic spallation cross sections", Phys. Rev. C 90 (2014) 064605

[188] N. Dubray, D. Regnier, "Numerical search of discontinuities in self-consistent potential energy surfaces", Comp. Phys. Comm. 183 (2012) 2035

[189] F. Rejmund, A. V. Ignatyuk, A. R. Junghans, K.-H. Schmidt, "Pair breaking and even-odd structure in fission-fragment yields", Nucl. Phys. A 678 (2000) 215

[190] M. Mirea, "Energy partition in low-energy fission", Phys. Rev. C 83 (2011) 054608

[191] N. Carjan, F.-J. Hambsch, M. Rizea, O. Serot, M. Mirea, "Partition between the fission fragments of the excitation energy and of the neutron multiplicity at scission in low-energy fission", Phys. Rev. C 85 (2012) 044601

[192] M. Brack, J. Damgaard, A. S. Jensen, H. C. Pauli, V. M. Strutinsky, C. Y. Wong, "Funny Hills: the shell-correction approach to nuclear shell effects and its Applications to the Fission Process", Rev. Mod. Phys. 44 (1972) 320

[193] S. Goriely, N. Chamel, J. M. Pearson, "Hartree-Fock-Bogoliubov nuclear mass model with 0.50 MeV accuracy based on standard forms of Skyrme and pairing functionals", Phys. Rev. C 88 (2013) 061302

[194] Adam Sobiczewski, Yuri A. Litvinov, "Accuracy of theoretical descriptions of nuclear masses", Phys. Rev. C 89 (2014) 024311

[195] P.-G. Reinhard, M. Bender, W. Nazarewicz, T. Vertse, "From finite nuclei to the nuclear liquid drop: Leptodermous expansion based on self-consistent mean- field theory", Phys. Rev. C 73 (2006) 014309

[196] I. Ragnarsson, R. K. Sheline, "Systematics of nuclear deformations", Phys. Scr. 29 (1984) 385

[197] N. Zeldes, T. S. Dumitrescu, H. S. Köhler, "Mutual support of magicities and residual effective interactions near ^{208}Pb", Nucl. Phys. A 399 (1983) 11

[198] V. M. Strutinsky, "Shells in deformed nuclei" Nucl. Phys. A 122 (1968) 1

[199] Peter Möller, Takatoshi Ichikawa, "A method to calculate fission-fragment yields Y(Z,N) versus proton and neutron number in the Brownian shape-motion model", Eur. Phys. J. A 51 (2015) 173

[200] S. G. Kadmensky, D. E. Lyubashevsky, L. V. Titova, "Angular and spin distributions of primary fission fragments", Bull. Russ. Academy Sciences: Physics 75 (2011) 989

[201] S. G. Kadmensky, L. V. Titova, "Problem of the conservation of the fissile-nucleus-spin projection onto the fissile-nucleus symmetry axis and quantum dynamics of the low-energy fission process", Phys. Atom. Nuclei 72 (2009) 1738

[202] P. G. Reinhard, private communication, 2013

[203] W. D. Myers, W. J. Swiatecki, "The congruence energy: a contribution to nuclear masses, deformation energies and fission barriers", Nucl. Phys. A 612 (1997) 249

[204] J. Sadhukhan, W. Nazarewicz, N. Schunk, "Microscopic modeling of mass and charge distributions in the spontaneous fission of 240Pu", Phys. Rev. C 93 (2016) 011304(R)

[205] H. Delagrange, S. Y. Lin, A. Fleury, J. M. Alexander, "Energy dependence of fissionability for ^{239}Pu, ^{238}Pu, and ^{241}Am", Phys. Rev. Lett. 39 (1977) 867

[206] S. Pommé, E. Jacobs, K. Persyn, D. De Frenne, K. Govaert, M.-L. Yoneama, "Excitation energy dependence of charge odd-even effects in the fission of ^{238}U close to the fission barrier", Nucl. Phys. A 560 (1993) 689